



OPEN

Species-specific metabolomic profiles of coral reef coralline algae and their influence on the larval settlement of corals and crown-of-thorns starfish

Guillermo Diaz-Pulido¹✉, Steven D. Melvin², Sophie Ferguson³, Andrea Severati³, Peter C. Doll⁴, Sven Uthicke³, Andrew P. Negri³ & Muhammad A. Abdul Wahab³

To address a significant knowledge gap in chemical ecology underpinning larval settlement processes on coral reefs, we examined the tissue-associated metabolomes using nuclear magnetic resonance (NMR) spectroscopy across 14 species of crustose coralline red algae (CCA) and one non-coralline calcareous red alga collected from the Great Barrier Reef, Australia. We further explored the relationship between algal metabolites and the settlement success of fifteen reef-building coral species across five families, as well as a key coral predator, the crown-of-thorns starfish (CoTS; *Acanthaster cf. solaris*). We found that algal metabolomes are highly variable and differ among species, phylogenetic lineages, and reef habitats, highlighting the combined influence of evolutionary history and environmental context on algal metabolomes. We also identified strong, positive correlations between specific algal metabolites, particularly disaccharides and trisaccharides (e.g., raffinose, maltose), and glycine betaine with high settlement success in both corals and CoTS. This study provides the most comprehensive analysis to date of coralline algal metabolomes and their ecological significance to coral reef ecosystems. These results provide novel chemical, biological and ecological insights that may be used to inform the optimisation of coral aquaculture techniques for reef restoration, as well as potential strategies for controlling CoTS outbreaks to mitigate ongoing reef decline.

Keywords *Acanthaster*, Chemical cues, Coral larval settlement, Crustose coralline algae, Great Barrier Reef, Reef restoration

Coral reef degradation has intensified due the cumulative impacts of warming-induced coral bleaching, ocean acidification, nutrient pollution, and outbreaks of key coral predators such as the crown-of-thorns starfish (CoTS). These pressures have caused widespread coral mortality and driven substantial shifts in reef structure and function^{1–3}. The degradation of coral reefs poses threats to biodiversity and the ecosystem services they provide, including fisheries production, coastal protection against storms, and opportunities for tourism and recreation – services essential for environmental health and human wellbeing⁴.

While reducing carbon dioxide emissions and strengthening management practices of reefs remain critical to halting long-term decline, it is also important to implement concurrent strategies that promote coral recovery and mitigate threats from outbreaks of coral predators. A fundamental process underpinning coral recovery is the settlement of planktonic coral larvae to the benthos to suitable hard substrates, a step widely recognised as being facilitated by coralline algae^{5–7}. Notably, larval settlement of coral-feeding CoTS (*Acanthaster spp.*) is also mediated by cues from coralline algae⁸, as is the case for other echinoderms⁹, abalone¹⁰ and other marine invertebrates¹¹. Crustose coralline algae (or CCA) are a distinctive group of red calcareous algae that deposit high magnesium calcite skeletons¹². As important reef builders and ecosystem engineers, they play a foundational role in reef construction and consolidation^{13–15}, as well as the formation of rhodolith, and maerl beds^{16,17}. Through

¹School of Environment and Science, Griffith University, Brisbane, QLD 4111, Australia. ²School of Environment and Science, Griffith University, Gold Coast, QLD 4069, Australia. ³Australian Institute of Marine Science, PMB No.3, Townsville, QLD 4810, Australia. ⁴College of Science and Engineering, James Cook University, Townsville, QLD 4811, Australia. ✉email: g.diaz-pulido@griffith.edu.au

these functions, coralline algae are integral to the resilience and recovery of marine populations and benthic communities.

The mechanisms by which CCA induce larval settlement are varied, although it is generally accepted that chemical cues play a central role. These cues may be produced directly by the algal tissue^{18,19}, by microbial communities associated with their surfaces^{20–22}, or by a combination of both, functioning as a holobiont²³. Some CCA such as *Titanoderma* spp. are consistently strong inducers of larval settlement across a range of coral taxa^{23–25}, while others can inhibit larval settlement²⁶. There are also species-specific interactions between CCA and invertebrate larvae, such as the coral *Fungia fungites* and species of the Lobophylliidae, which settle preferentially on the CCA *Sporolithon* sp.²⁵, and CoTS larvae which preferentially settle on *Melyvonnea cf. madagascariensis*⁸. Understanding the chemical profiles of CCA is not only valuable for ecological insights but also holds practical applications for coral aquaculture and reef restoration, where enhancing larval settlement is a key objective^{27,28}. In the case of CoTS, identifying CCA metabolites associated with preferred or avoided CCA substrates may provide insight into settlement processes and recruitment patterns, potentially informing management of population outbreaks that have devastated coral populations across the Indo-Pacific^{1,29,30}.

Despite their ecological importance, our understanding of CCA chemical profiles, specifically their metabolomes (the complete set of metabolites within an organism), remains limited, and only a handful of species' metabolomes have been studied to date^{23,27,31,32}. However, emerging research has shown that CCA possess one of the most chemically complex and diverse metabolomes of coral reef benthic organisms, surpassing even reef-building corals, algal turfs and fleshy macroalgae^{33,34}. Although many unique compounds have been detected, the majority remain unidentified^{31,33,34}. Jorissen et al.²³ and Vizon et al.³² compared the metabolomes of six and seven CCA species, respectively, from French Polynesian reefs, and found substantial variation in metabolomic profiles across species and reef microhabitats. However, their studies covered a limited number of taxa, leaving open questions about how consistent tissue-associated metabolite profiles are across a broader array of CCA, and whether these profiles reflect phylogenetic relationships. Furthermore, the role of specific metabolites or metabolomic signatures in inducing larval settlement of marine invertebrates remains poorly understood³⁵. While some progress has been made in identifying classes of compounds potentially involved (e.g. betaine lipids), there is a clear need for systematic metabolomic characterisation using methods such as H-NMR across taxonomic groups and ecological contexts²³. Given the high diversity of coralline algae species, with more than 1,111 taxa reported worldwide³⁶ and their distinct ecological functions (species can have different ecological functions in a coral reef system, e.g. larval settlement induction, reef cementation, framework building), elucidating species-specific and phylogenetically informed metabolomic patterns is essential.

The main objectives of this study are:

- First, to determine whether tissue-associated metabolomes differ among coral reef CCA by comparing the composition and abundance of metabolites across 14 species of coralline algae and one non-coralline red calcareous alga. This will help identify species-specific chemical profiles and key metabolites.
- Second, to examine the relationship between phylogenetic affiliation and metabolic composition by analysing whether metabolomes are conserved within taxonomic orders or families, thus exploring potential evolutionary patterns in metabolic traits.
- Third, to assess whether metabolic profiles vary across reef environments (i.e. habitats and light environments), providing insight into the extent to which environmental conditions shape CCA metabolomes.
- Finally, to explore which CCA metabolites are positively or negatively correlated with larval settlement success for 15 species of reef-building corals and western Pacific CoTS (*Acanthaster cf. solaris*), thereby generating testable hypotheses about settlement cues.

Results

Nuclear Magnetic Resonance (NMR) spectroscopy analyses of 14 CCA species and one red calcareous alga species (Table 1) detected a total of 71 chemical features (or putative metabolites) associated with the algal tissues. Of these, 28 metabolites were confidently identified, with an additional 10 features tentatively annotated (Supplementary Table S1). The remaining 33 features (46%) could not be assigned to known metabolites or chemical classes (Supplementary Table S2), highlighting the presence of novel or uncharacterised compounds in these algal taxa. The identified metabolites spanned several chemical classes, including: organooxygen compounds (carbohydrates such as monosaccharides, oligosaccharides, O-glycosyl), organonitrogen compounds (e.g. quaternary ammonium salts such as choline and aminoxides like TMAO); carboxylic acids and derivatives (e.g. amino acids, peptides and analogues); lipids and lipid-like molecules (fatty acyls, possibly fatty acyl glycosides); alkaloids and derivatives; and nucleosides and nucleotide analogues (Supplementary Table S1).

Variability of metabolomes among CCA species

Multivariate analyses of both identified and unknown metabolites revealed a clear separation between CCA samples and the aragonite substrate controls (Supplementary Fig. S1). In this comparison, the first two principal components (PC1 and PC2) explained 53.6% of the total variance (Supplementary Fig. S1). When aragonite controls and algal turf treatments were excluded, the refined PCA improved the separation of samples by CCA species, though separation was not complete, with PC1 and PC2 together accounting for 50.2% of the variance (Fig. 1a; Supplementary Table S3 for PERMANOVA pairwise comparisons). Samples from *Ramicrusta* sp., *Sporolithon* sp., and *Lithothamnion cf. proliferum* formed distinct clusters, whereas other species showed greater overlap in their metabolic profiles.

To further resolve species-level groupings, we applied a partial least squares discriminant analysis (PLS-DA) which enhanced species-specific clustering and revealed additional patterns, such as a distinct grouping of

| Species | Species abbreviation | Family/ Sub-family | Order | Collection site | Habitat | Irradiance level | No. fragments (herbarium specimens) | Herbarium numbers | GenBank psbA | GenBank rbcL |
|---|----------------------|---------------------|-----------------|-------------------|-------------------|-----------------------|-------------------------------------|-------------------|--------------|--------------|
| <i>Adeylithon cf. bosencei</i> | Ab | Hydrolithoideae | Corallinales | Davies Reef | Shallow reef, 4 m | High | ca. 180 (3) | DP-2438 | OP830454 | OP830469 |
| <i>Amphiroa cf. foliacea</i> | Af | Lithophylloideae | Corallinales | Davies Reef | Shallow reef, 4 m | Moderate (mid-high) | ca. 180 (3) | DP-2437 | OP830453 | OP830468 |
| <i>Hydrolithon cf. reinboldii</i> | Hr | Hydrolithoideae | Corallinales | Palm Island Group | Shallow reef, 4 m | Moderate (mid) | ca. 200 (14) | DP-2526 | OP830457 | OP830472 |
| <i>Lithophyllum cf. kotschyannum</i> | Lk | Lithophylloideae | Corallinales | Davies Reef | Shallow reef, 4 m | High | 239 (5) | DP-2434 | OP830451 | OP830466 |
| <i>Lithophyllum cf. insipidum</i> | Li | Lithophylloideae | Corallinales | Palm Island Group | Shallow reef, 2 m | High | 150 (4) | DP-2559 | OP830456 | OP830471 |
| <i>Lithophyllum cf. pygmaeum</i> | Lpy | Lithophylloideae | Corallinales | Davies Reef | Shallow reef, 4 m | Moderate (mid – high) | ca. 180 (16) | DP-2430 | OP830449 | OP830464 |
| <i>Lithothamnion cf. proliferum</i> | Lpr | Hapalidiaceae | Hapalidiales | Davies Reef | Caves, crevices | Low | 226 (4) | DP-2428 | OP830448 | OP830463 |
| <i>Melyvonnea cf. madagascariensis</i> | Mm | Mesophyllumaceae | Hapalidiales | Davies Reef | Shallow reef, 6 m | Moderate (low – mid) | 127 (10) | DP-2493; DP-2436 | OP830452 | OP830467 |
| <i>Neogoniolithon cf. fosliei</i> | Nf | Neogoniolithoideae | Corallinales | Davies Reef | Reef crest | High | 262 (2) | DP-2489-2 | OP830450 | OP830465 |
| <i>Porolithon onkodes</i> “chalky” | Pon | Metagoniolithoideae | Corallinales | Davies Reef | Reef crest | High | ca. 180 (4) | DP-2425 | OP830445 | OP830460 |
| <i>Porolithon</i> sp. “orange” | Por | Metagoniolithoideae | Corallinales | Davies Reef | Reef crest | High | ca. 180 (9) | DP-2423 | OP830444 | OP830460 |
| <i>Porolithon</i> sp. “yellow conceptacles” | Poy | Metagoniolithoideae | Corallinales | Palm Island Group | Reef crest | High | 180 (13) | DP-2467 | OP830446 | OP830461 |
| <i>Ramicrusta</i> sp. | Ra | Peyssonneliaceae | Peyssonneliales | Davies Reef | Caves, crevices | Low | 219 (3) | DP-2435 | OP830458 | OP830473 |
| <i>Sporolithon</i> sp. | Sp | Sporolithaceae | Sporolithales | Davies Reef | Caves, crevices | Low | > 185 (10) | DP-2439 | OP830455 | OP830470 |
| <i>Titanoderma cf. tessellatum</i> | Tt | Lithophylloideae | Corallinales | Davies Reef | Shallow reef, 4 m | Low - mid | 443 (10) | DP-2427 | OP830447 | OP830462 |

Table 1. List of 14 species of coralline algae and one species of calcareous red algae (*Ramicrusta*) used in the study with abbreviation used in figures, taxonomic classification (family, orders), collection site, habitat and irradiance level, number of fragments collected from the field and herbarium specimens (in brackets) retained in the Coral Reef Algae Lab collection of Diaz-Pulido at Griffith University, Australia. GenBank accession numbers for representative psbA and rbcL sequences of each algal species are included.

Porolithon spp. (Fig. 1b). The PLS-DA model was validated showing a $Q_2 = 0.43$ ($R^2 = 0.52$; $p < 0.001$), indicating moderate predictive power, perhaps constrained by the large number of species included.

To refine separation and reduce the influence of less informative variables (by reducing the number of metabolites from the dataset), a sparse partial least squares discriminant analysis (sPLS-DA) was conducted. This analysis identified a clear separation of *Neogoniolithon* cf. *fosliei* samples from other CCA species, in addition to those already grouped by the PLS-DA (e.g. *Sporolithon* sp.) (Fig. 1c). While these multivariate approaches revealed species-specific patterns in metabolomic profiles, substantial overlap among taxa remained, and full resolution was not achieved. To discern whether closely related species within genera (e.g., *Porolithon* and *Lithophyllum*) possess distinct chemical profiles, we performed sPLS-DA within each genus (Supplementary Fig. S2). These within-genus analyses supported the separation of metabolite profiles at the species level (Supplementary Fig. S2).

To identify metabolites that are driving the separation among species profiles we examined variable importance in projection (VIP) scores and loading plots from the PLS-DA and sPLS-DA models respectively (Supplementary Fig. S3a, b). Most high-ranking VIP compounds were uncharacterised (e.g., unknown40, unknown14). To further examine species enrichment of known metabolites, we generated heatmaps of relative metabolite concentrations across CCA species (Fig. 2). Distinct patterns of metabolite enrichment were evident among species. For example, *Ramicrusta* sp. was particularly enriched in several known metabolites, including pyroglutamate, leucine, glutamic acid, citrulline, putative glycerate (unknown18), and a putative 5-Dodecenioic acid (unknown8), along with multiple unknowns than could not be annotated (Fig. 2). *Neogoniolithon* cf. *fosliei* was enriched in pseudouridine, leucine, valine, isoleucine, glycyproline and uridine. Species of *Porolithon*, which clustered together, were high in uridine, putative acetylserine and several unknown metabolites. *Sporolithon* sp. was only enriched in TMAO and was particularly low in glycyproline, trehalose and quinone, suggesting the simplest metabolomic signature among the studied taxa. A shared enrichment pattern of phenylalanine, formic acid, and trigonelline was observed in *Melyvonnea* cf. *madagascariensis* and *Hydrolithon* cf. *reinboldii* (Fig. 2). The latter species, along with *Lithophyllum* cf. *insipidum*, also showed elevated levels of maltose and raffinose.

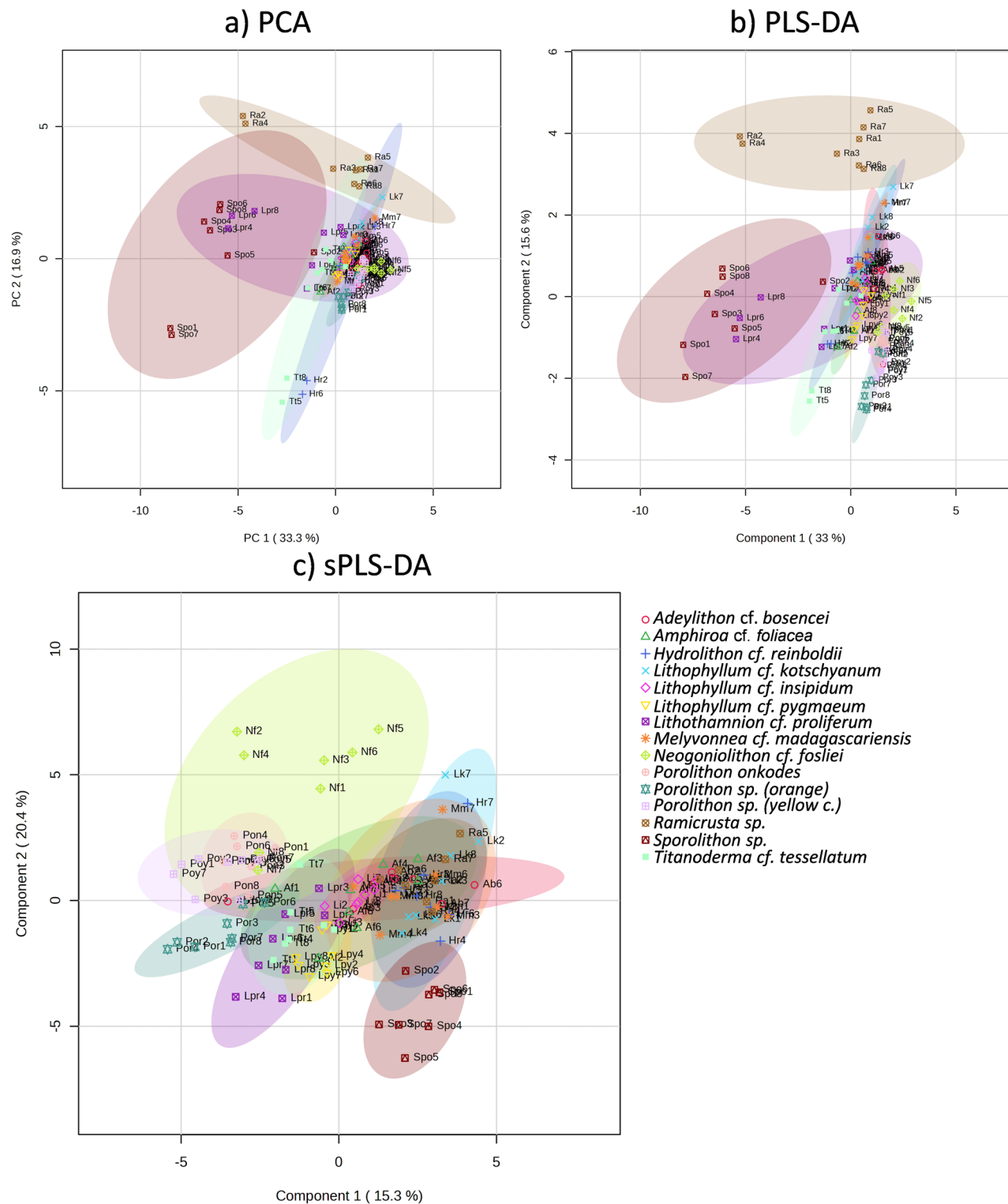


Fig. 1. Multivariate analyses of metabolic profiles in 14 species of coralline algae and one species of red calcareous alga (*Ramicrusta* sp.). (a) Principal Component Analysis (PCA); (b) Partial least squares discriminant analysis (PLS-DA); (c) Sparse partial least squares discriminant analysis (sPLS-DA). Figures with overlapping sample names abbreviated as indicated in Table 1. Symbols represent samples and colours the species. Ellipses display 95% confidence regions. PERMANOVA F -value: 15.236; PC on X-axis: 1, PC on Y-axis: 2, explaining 33.3 and 16.9% of the variance, respectively (total variance explained: 50.2%); R^2 : 0.67013; $p=0.001$. Distributions are computed using the Euclidean distance. PLS-DA: $Q^2=0.43$, $R^2=0.52$; $p<0.001$ (1,000 permutations). sPLS-DA was run with 5 components and 10 variables within each component, with Classification Error Rate for two components = 23%.

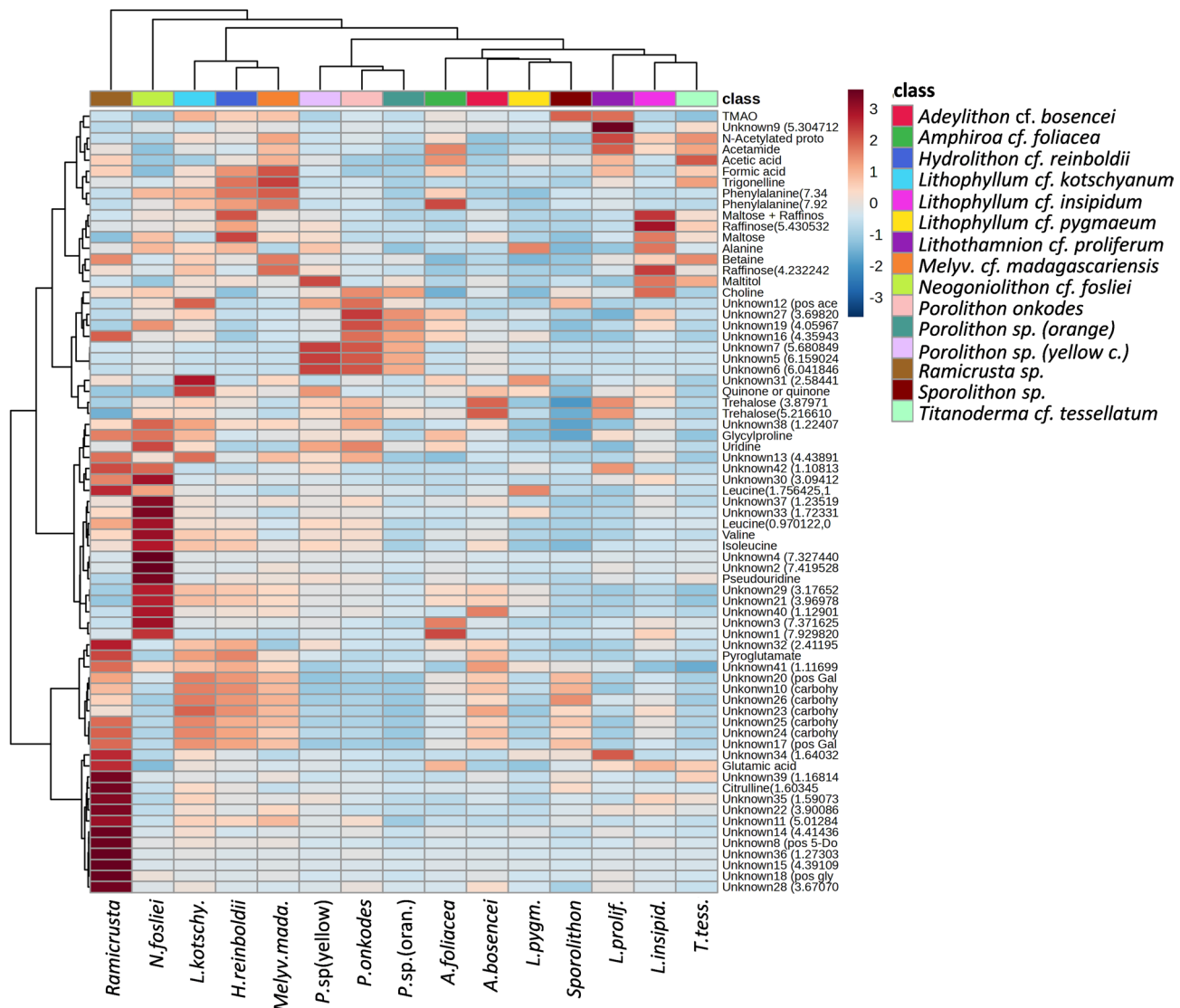


Fig. 2. Heatmap showing the relative concentration of metabolites (in rows) among coralline algae and *Ramicrusta* (in columns). Values are group averages (by samples, $n=8$) of normalised intensity of features. Clustering was performed using Euclidean distance. Heatmap includes unknown metabolites (features).

In contrast, *Titanoderma cf. tessellatum* had no metabolites ranked as VIPs and was overall characterised by low metabolite loadings relative to other species (Supplementary Fig. S3a, b).

Relationship between CCA metabolomes and CCA phylogeny

To investigate whether phylogenetic affinities among coralline algae (Subclass Corallinophycidae) correspond to similarities in metabolic profiles, we conducted multivariate analyses excluding the order Peyssonneliales, which belongs to a different subclass of red algae (Rhodymeniophycidae). The sPLS-DA revealed a correspondence between metabolic profiles and the phylogenetic arrangement of Corallinophycidae, both at the order (i.e. Corallinales, Hapalidiales, and Sporolithales) and family levels (Fig. 3a, b; Supplementary Fig. S4). The three orders formed distinct clusters, with Sporolithales particularly well segregated. PERMANOVA pairwise comparisons from Principal Component Analyses (PCA) showed significant differences among orders (Supplementary Table S4). At the family level, clear distinctions were observed among Sporolithaceae (Sporolithales), Hapalidiaceae (Hapalidiales), and both Neogoniolithoideae and Metagoniolithoideae (Corallinales). In contrast, substantial overlap in metabolic profiles was evident among Mesophyllumaceae (Hapalidiales), Hydroolithoideae and Lithophylloideae (Corallinales), with no clear separation between these families (Fig. 3b), observations supported by PERMANOVA pairwise comparisons (Supplementary Table S4).

VIP analysis identified several unknown compounds (Unknown40, 33, 32, 19) that drove the clustering of samples by orders and families (Supplementary Fig. S3c-f). Twelve VIP compounds were enriched in Corallinales, while only one was enriched in Sporolithales (i.e. Trimethylamine N-oxide -TMAO) (Supplementary Fig. S3c, d). Compounds enriched in Corallinales include leucine, pyroglutamate, valine and alanine, while glutamic

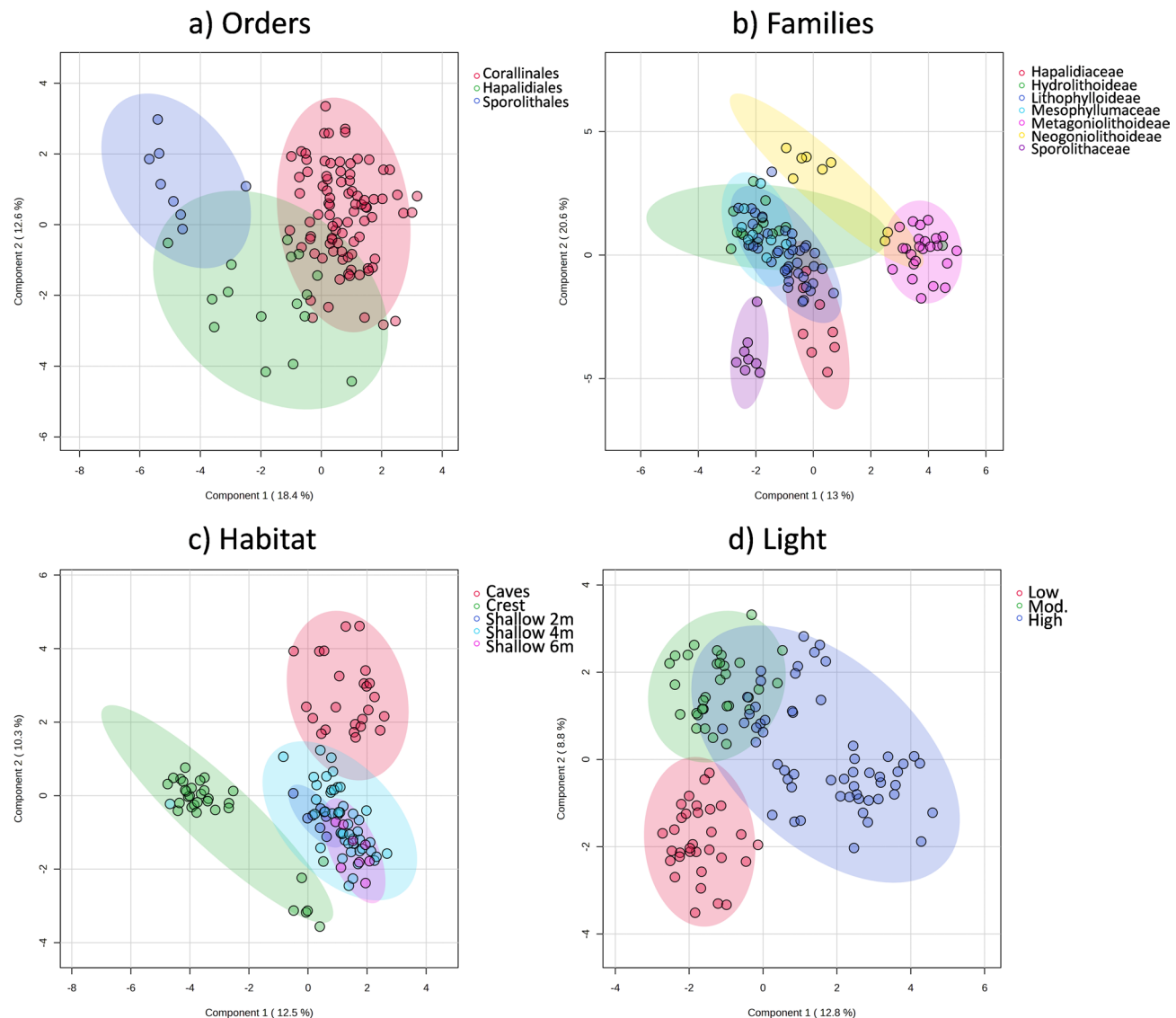


Fig. 3. Relationship between coralline algae metabolic profiles, phylogeny and the environment. Sparse Partial Least Squares Discriminant Analysis (sPLS-DA) of metabolite profiles in 14 coralline algae species grouped by their phylogenetic classification of (a) Order; (b) Family, both excluding *Ramicrusta* sp. (Peyssonneliales) samples; and (c) Habitat; and (d) Light environment, both including *Ramicrusta* sp. Symbols represent samples and colours the groupings. Samples from aragonite substrates and algal turfs are excluded. Ellipses display 95% confidence regions. sPLS-DA were run with 5 components and 10 variables within each component and Classification Error Rates for two components were 3.6, 18.8, 11.7 and 7.5% for (a–d), respectively. PERMANOVA pairwise comparisons from Principal Component Analyses (PCA) for the variables considered are presented in (Supplementary Table S4).

acid, acetic acid, phenylalanine, formic acid, and trigonelline, among others, were enriched in Hapalidiales (Supplementary Fig. S4a). Although few VIPs were associated with Sporolithales, this order showed enrichment in citrulline, TMAO, choline and a range of unknown carbohydrates (Supplementary Fig. S4a).

Several VIPs also contributed to the separation at the family level (Supplementary Fig. S3e). *Metagoniolithoideae* was enriched in three unknown compounds (e.g. Unknown6, 7, and 5), while choline was also elevated, though it had a low VIP score. *Neogoniolithoideae* showed enrichment in four unknown metabolites (e.g. Unknown40 and 19), as well as leucine, valine, and isoleucine (all with low VIP scores). *Mesophyllumaceae* was enriched in one unknown carbohydrate and several low-VIP compounds including phenylalanine, trigonelline, betaine (also known as glycine betaine) and raffinose (Fig. 2; Supplementary Fig. S3e, f). Interestingly, *Lithophylloseae* showed no strongly enriched VIPs; only Unknown31 was moderately enriched, although it had a low VIP score (Supplementary Fig. S4b).

Relationship between CCA metabolomes and reef habitat and light environments

The metabolic profiles of the CCA also reflected the reef habitats and light environments from which samples were collected. The sPLS-DA grouped samples according to habitat, with a clear separation of samples from reef crest and cave habitats, and an intermediate grouping from shallow to moderate depths (Fig. 3c; Supplementary Table S4 for PCA PERMANOVA pairwise comparisons). Samples also clustered by the light environment, with clear separation between low and high irradiance settings, with samples from moderate irradiance partially overlapping with those from high light (Fig. 3d; Supplementary Table S4). PLS-DSA models also demonstrated good predictive ability, with two component models for both habitat and light environment yielding Q2 values of 0.632 ($R^2 = 0.657, p < 0.001$) and 0.664 ($R^2 = 0.722, p < 0.001$), respectively.

Known metabolites such as trehalose, uridine, valine, glycylproline, leucine, putative acetylserine (unknown12), pseudouridine, and isoleucine were enriched in CCA samples from the shallow reef crest habitat (Supplementary Fig. S5a, heatmap). In addition, seven unidentified VIPs (unknown6, 7, 5, 19, 33, 37) and trehalose were also highly enriched in this habitat (Supplementary Fig. S6a). In contrast, citrulline and 11 unknown metabolites were elevated in samples from caves/overhang habitats (Supplementary Fig. S5b), with VIP scores highlighting two unidentified compounds (unknown39, 34) and a putative glycerate (unknown18) feature as cave-associated (Supplementary Fig. 6a). Metabolites enriched in well-lit environments included leucine 0.9701, maltitol, choline, glycylproline, trehalose, pseudouridine, valine, isoleucine, raffinose, uridine (Supplementary Fig. S5b). In contrast, betaine, leucine 1.7564, citrulline, glutamic acid, TMAO, and others were elevated under low light conditions (Supplementary Fig. S5b). VIPs associated with high-light environments included unknown features (unknown40, 6, 7, 5, 37, 19, 33), trehalose, quinone, choline, while only two VIPs were enriched under low light levels (unknown34, 39) (Supplementary Fig. 6c).

Relationship between CCA metabolomes and coral and CoTS settlement

Corals

The relationship between the CCA metabolomes and settlement in 15 coral species was assessed using total settlement (i.e. all coral species), family-level settlement (Acroporidae, Merulinidae, Lobophylliidae, Poritidae, and Fungiidae), and species-level settlement (Table 3 from Abdul Wahab et al. 2023). For clarity, we focussed on total and family-level settlement patterns, and on a subset of species where trends were most apparent.

Metabolic profiles differed significantly among the total settlement ranks (minimum, moderate and high; PERMANOVA F-value: 14.514; $R^2: 0.17915, p = 0.001$; Supplementary Table S5). While separation between moderate and high settlement profiles was less distinct, it remained statistically significant (PERMANOVA pairwise comparisons, $R^2 = 0.065, p$ adjusted = 0.004, Fig. 4a; Supplementary Table S5). Low total settlement corresponded to the aragonite substrates and, to a lesser extent, with profiles of *Amphiroa cf. foliacea*. The correspondence between settlement intensity varied across coral families and species. For example, species in the genus *Acropora*, such as *A. hyacinthus* showed a clear alignment, with settlement corresponding to distinct CCA metabolomic profiles, while in other corals such as *Platygyra sinensis*, that correspondence was less clear (Fig. 4).

Spearman rank correlations between relative metabolite concentrations (spectral bins) and total, family-level, and species-level settlement, showed that both the direction and intensity of the relationship varied according to the metabolites and taxonomic resolution examined (Supplementary Fig. S7). Several metabolites were positively correlated with total coral settlement, including raffinose (spearman rank correlation coefficient $r_s = 0.698, p < 0.0001, n = 136$, Fig. 5a), betaine ($r_s = 0.598, p < 0.0001$, Fig. 5b), maltose + raffinose ($r_s = 0.596, p < 0.0001$, Fig. 5c) and maltitol ($r_s = 0.48, p < 0.0001$, Fig. 5d), among others. These metabolites (raffinose 4.2322, raffinose 5.4305, betaine) also had high VIP scores (Supplementary Fig. S8). Heatmap of all relative metabolite concentrations across total settlement ranks (low to high) is shown in Supplementary Figure S9. Settlement within the Acroporidae was also positively correlated with raffinose 5.4305, maltose + raffinose, raffinose 4.2322, maltitol, betaine, and alanine (although the relationship is somewhat linear for alanine, Fig. 6a), and inversely correlated with TMAO (Supplementary Fig. S7b). The Poritidae, represented by *Porites lobata*, showed metabolite-settlement associations similar to those observed in Acroporidae (Supplementary Fig. S7e). For Merulinidae, positive correlations were observed with two raffinose metabolites, maltose + raffinose, betaine and several unknown compounds (Supplementary Fig. S7c). Notably, for *Mycedium elephantotus*, the relationship between raffinose 5.4305, and settlement deviated from a linear trend, with peak settlement occurring at intermediate raffinose concentrations (Fig. 6b).

In the Lobophylliidae, settlement was strongly associated with an unknown metabolite (unknown22; Spearman $r_s = 0.669, p < 0.0001$), in addition to two raffinose metabolites and betaine, the latter again exhibiting an apparent non-monotonic relationship (Fig. 6c). Metabolites that were positively correlated with settlement of Fungiidae included a putative galactose (unknown17, $r_s = 0.514, p < 0.001$) and several unknown carbohydrates. However, in contrast to other families, several metabolites were negatively correlated with settlement, including trehalose 5.2166 ($r_s = -0.399, p < 0.001$), quinone ($r_s = -0.392, p < 0.001$) and additional unknown compounds (Fig. 6d; Supplementary Fig. S7f).

CoTS

A statistically significant relationship was observed between the metabolic profiles of CCA species and CoTS larval settlement (PCA, PERMANOVA F-value: 6.4763; $R^2: 0.17397, p = 0.001$). Metabolic profiles from samples that corresponded with low settlement differed significantly from those with high and very high settlement (PERMANOVA pairwise comparisons, $R^2 = 0.355$ and $0.239, p$ adjusted = 0.005, 0.025 respectively). Although samples corresponding to low settlement clustered distinctly, there was no consistent or characteristic metabolic profile related to high settlement. Instead, high CoTS settlement appeared to result from a combination of diverse metabolic profiles, as indicated by the considerable overlap in CCA metabolomes across settlement categories

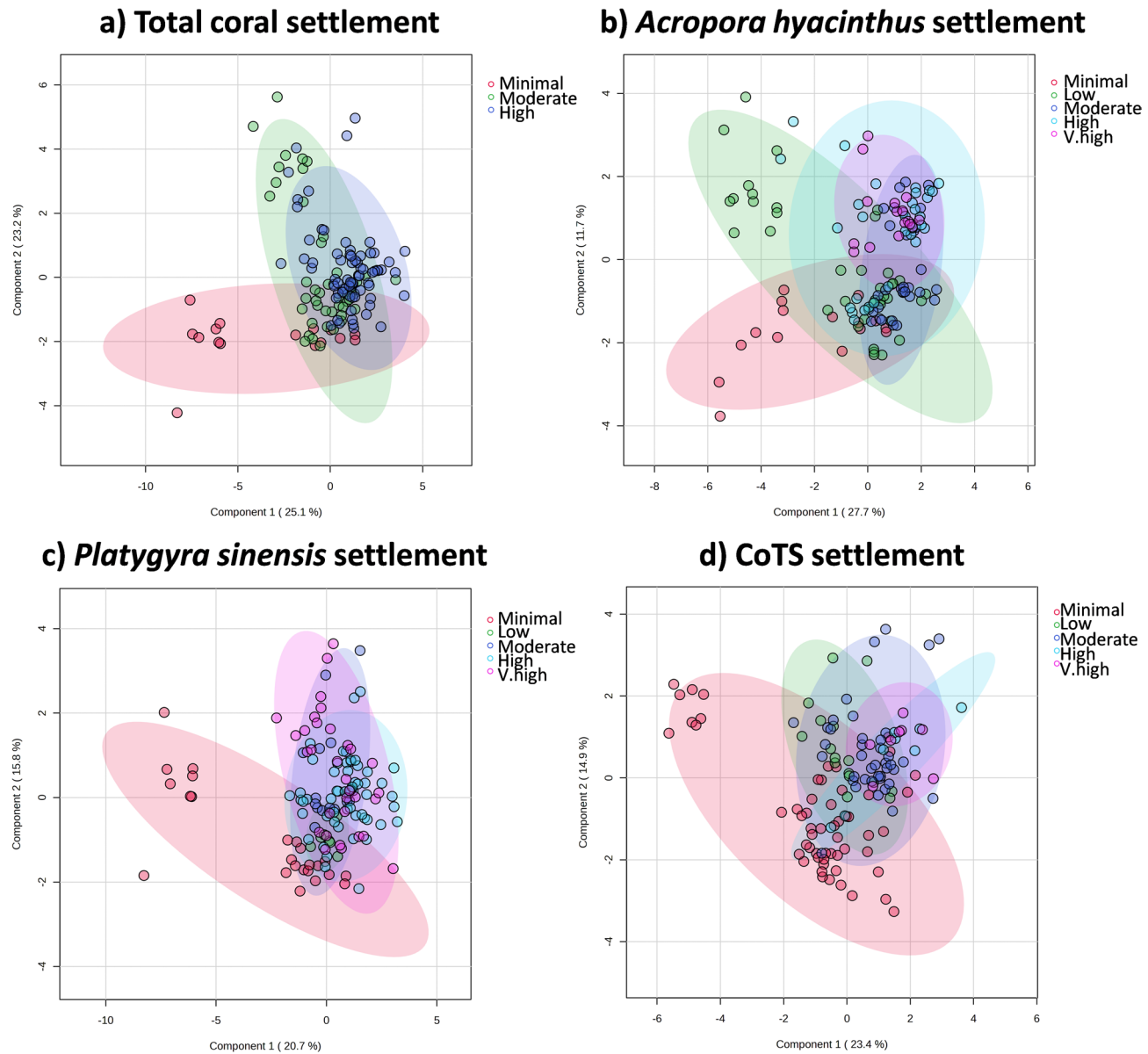


Fig. 4. Relationship between coralline algae metabolic profiles and larval settlement. Partial least squares discriminant analysis (PLS-DA) of metabolite profiles in 14 species of coralline algae and one species of red calcareous alga (*Ramicrusta*) grouped by settlement ranks of (a) Total coral (total larvae settled for all 15 coral species); (b) *Acropora hyacinthus*; (c) *Platygyra sinensis*; and (d) Crown-of-thorns starfish (CoTS). Symbols represent samples and colours the groupings. Ellipses display 95% confidence regions. Q2, R2 and p values (1,000 permutations) for (a–d) were 0.402, 0.461, < 0.001 ; 0.393, 0.481, < 0.001 ; 0.386, 0.483, < 0.001 ; and 0.4334, 0.504, < 0.001 , respectively. Settlement data was converted to a categorical, semiquantitative ranking (i.e. 0–19% = minimal; 20–39% = low, 40–59% = moderate, 60–79% = high, 80–100% = very high (V.high)); note that for Total settlement there are only 3 categories as those not included had a frequency of zero.

(PLS-DA shown in Fig. 4d). The VIP scores (Supplementary Fig. S8b) identified several compounds that have a large influence on the model arrangement, including a putative galactose (unknown20), which was enriched in high settlement samples. However, overall enrichment of VIP metabolites associated with high settlement was limited. One unknown compound (unknown7) was consistently high in samples that had low settlement, suggesting it may exert an inhibitory effect on CoTS settlement. A comprehensive heatmap displaying relative metabolite concentrations across settlement ranks is included in Supplementary Figure S9b.

To further explore these relationships, Spearman rank correlations were conducted between relative metabolite concentrations and CoTS settlement. Positive correlations were observed for maltose (Spearman $r_s = 0.571, p < 0.0001, n = 136$), maltose + raffinose ($r_s = 0.46, p < 0.0001$) and phenylalanine ($r_s = 0.454, p < 0.0001$), while citrulline was negatively correlated with settlement ($r_s = -0.354, p = < 0.001$) (Fig. 7; Supplementary Fig.

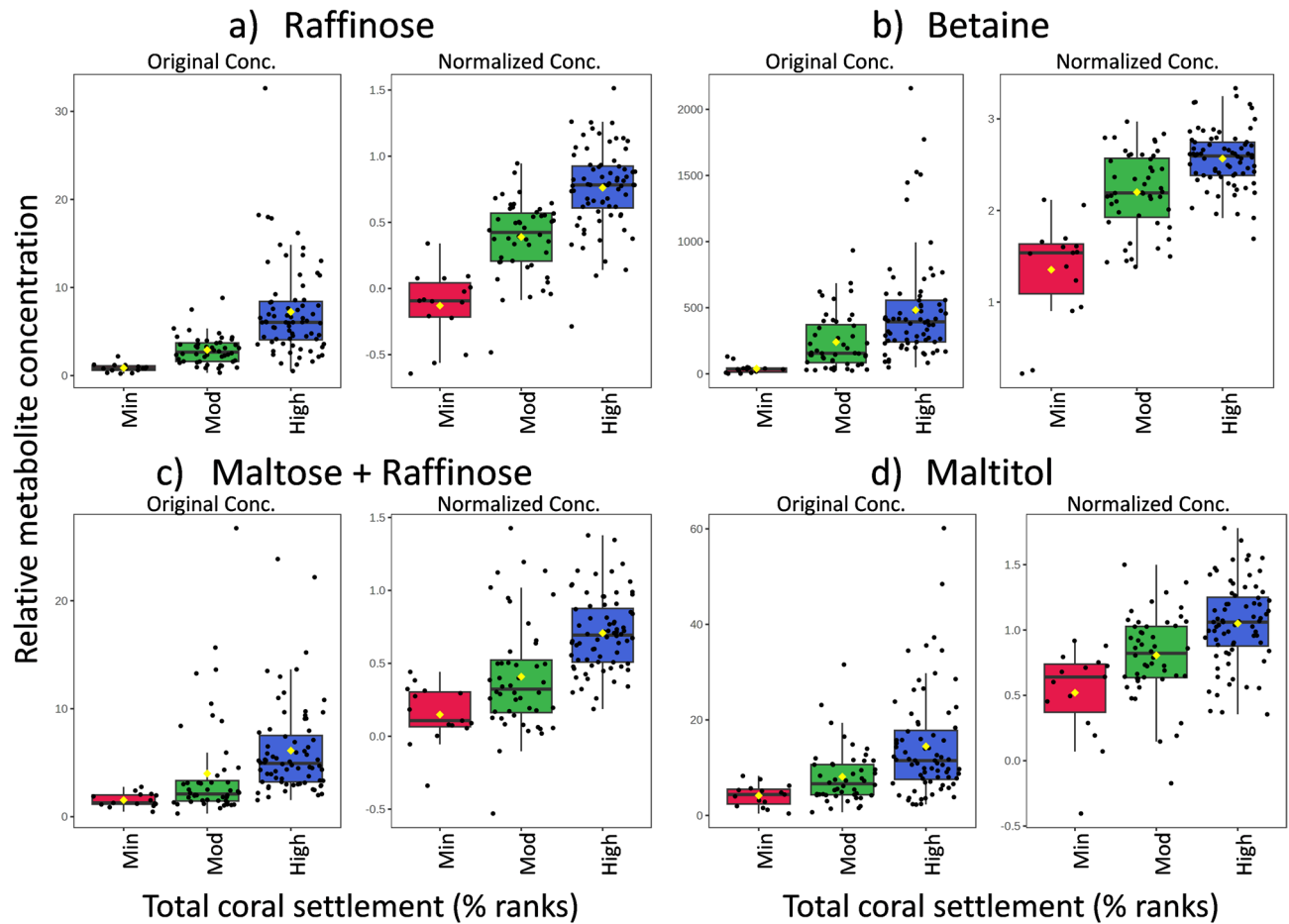


Fig. 5. Boxplots of relative concentrations (spectral bins) of metabolites across a gradient of Total coral settlement. **(a)** Raffinose (4.232242, 4.224698); **(b)** Betaine; **(c)** Maltose + Raffinose; and **(d)** Maltitol (possible annotation). Bar plots on the left show the original values (mean \pm SD) and the box and whisker plots on the right show the normalised values. Minimal: Min; Moderate: Mod. All metabolites are significantly correlated with settlement ranks (see text for details).

S7n, also heatmap in Supplementary Figure S9b). Notably, phenylalanine7.34 was particularly enriched in *Melyvonnea cf. madagascariensis* (Figs. 2 and 7d), suggesting a potential species-specific cue.

Discussion

This study explored the variability in metabolomes of coralline algae, a group of organisms critically important for coral reef resilience, using the most comprehensive dataset of coralline algae species examined to date. With this novel information, we investigated the relationship between algal metabolites and the settlement intensity of fifteen reef-building coral species across five families, as well as the settlement of a key coral predator, the crown-of-thorns starfish (*Acanthaster cf. solaris*). Our findings revealed that CCA metabolomes are highly variable and differ among species, phylogenetic lineages, and reef habitats, highlighting the combined influence of evolutionary history and the environmental context on algal metabolomes. We also identified strong, positive correlations between specific metabolites, particularly disaccharides and trisaccharides (e.g., raffinose, maltose), and amino acid derivatives (e.g. betaine), to high settlement in corals and CoTS. Together, these results provide novel chemical, biological and ecological insights that can inform the optimisation of coral aquaculture techniques for reef restoration, as well as strategies for controlling CoTS outbreaks to help halt ongoing reef decline.

Variability among CCA species and characteristic metabolites

The metabolic profiles of the studied coralline algae varied significantly between species, although there was considerable overlap between some profiles. *Neogoniolithon cf. fosliei*, *Sporolithon* sp., and the non-coralline calcareous alga *Ramicrusta* sp. had clearly differentiated chemical signatures. Many of the VIP compounds driving the uniqueness in chemical profiles remain unidentified. While, certain metabolites were enriched across multiple species, they were not diagnostic (i.e. VIP compounds) of individual taxa. Our findings are consistent with the results from two other comparative metabolomics studies of coralline algae, both conducted in French Polynesia^{23,32}, which similarly demonstrated that coralline algae possess species-specific metabolomes. Jorissen

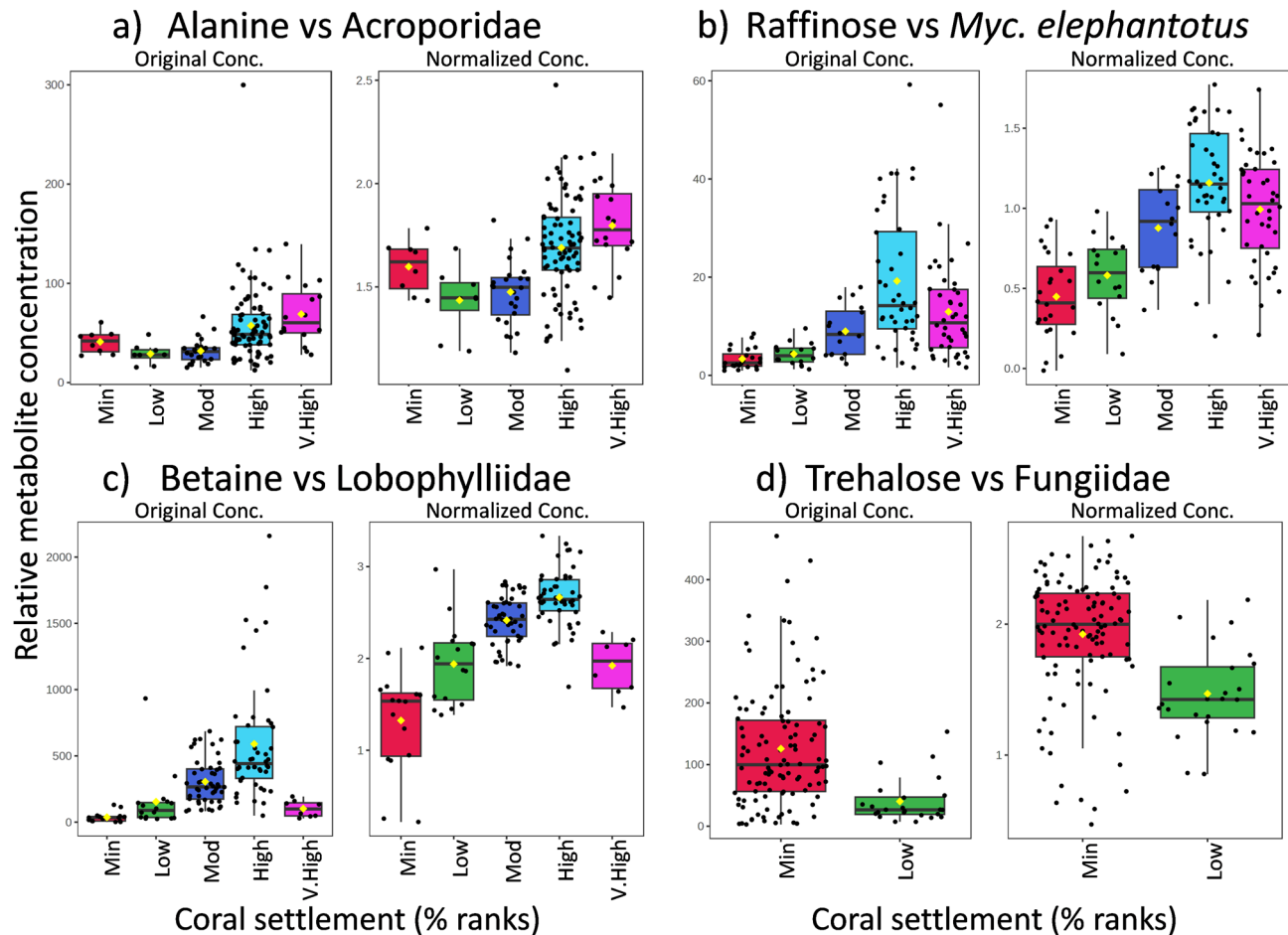


Fig. 6. Boxplots of relative concentrations (spectral bins) of metabolites across a gradient of coral larval settlement. **(a)** Alanine vs. Acroporidae settlement; **(b)** Raffinose (5.4305) vs. *Mycedium elephantotus*; **(c)** Betaine vs. Lobophylliidae settlement; and **(d)** Trehalose (5.2166) vs. Fungiidae settlement. Bar plots on the left show the original values (mean \pm SD) and the box and whisker plots on the right show the normalised values. All metabolites are significantly correlated with settlement (see text for details).

et al. (2021) identified fifteen VIP compounds characteristic of *Titanoderma*, all of which were glycerolipids, including four betaine lipids. In contrast, our study did not identify any VIP compounds in relative high concentrations uniquely associated with *Titanoderma cf. tessellatum*. On the contrary, the metabolome of *T. cf. tessellatum* was characterised by generally low relative metabolite concentrations compared to other species (based on inspection of Heatmap in Fig. 2; Supplementary Fig. S3a, b). Although betaine (known as glycine betaine) was moderately enriched in *T. cf. tessellatum*, it did not emerge as a defining compound (Supplementary Fig. S3). Similarly, *Sporolithon* exhibited widespread depletion of metabolites, underscoring the broad chemical diversity and distinctiveness of CCA metabolomes.

The metabolome of the calcareous, non-CCA red alga *Ramicrusta* sp. was also clearly distinct from those of the CCA examined, which is consistent with its classification outside the coralline algae (Corallinophycidae). A previous study from the Caribbean found caffeine enriched in exudates from a *Ramicrusta* species³⁷; however, caffeine was not detected in our samples. Other shared metabolites such as phenylalanine, were present in both datasets. Although *Neogoniolithon cf. fosliei* also displayed a highly distinctive metabolomic profile in our study, limited comparative data are available to place this finding in a broader context.

Relationship of metabolomes with phylogenetic groups

The metabolic profiles of coralline algae reflected the phylogenetic organization of the Corallinophycidae, which was particularly evident at the order level and, to some extent at the family level. As with species-level analysis, the majority of compounds responsible for the unique signatures of specific groups are unknown, which limits detailed interpretation. However, some clear patterns emerged.

The order Sporolithales exhibited a highly distinct metabolic profile, characterised by a single VIP feature – the organonitrogen compound TMAO. Sporolithales represents the most ancient lineage within the Corallinophycidae, with an estimated divergence dating back to the Lower Cretaceous (~ 137 million years ago (Ma))^{38,39}. In contrast, Corallinales, is the most recently evolved order (ca. 66 Ma), with intermediate divergence in Hapalidiales (116 Ma). It has been proposed that more ancient or morphologically simpler plant

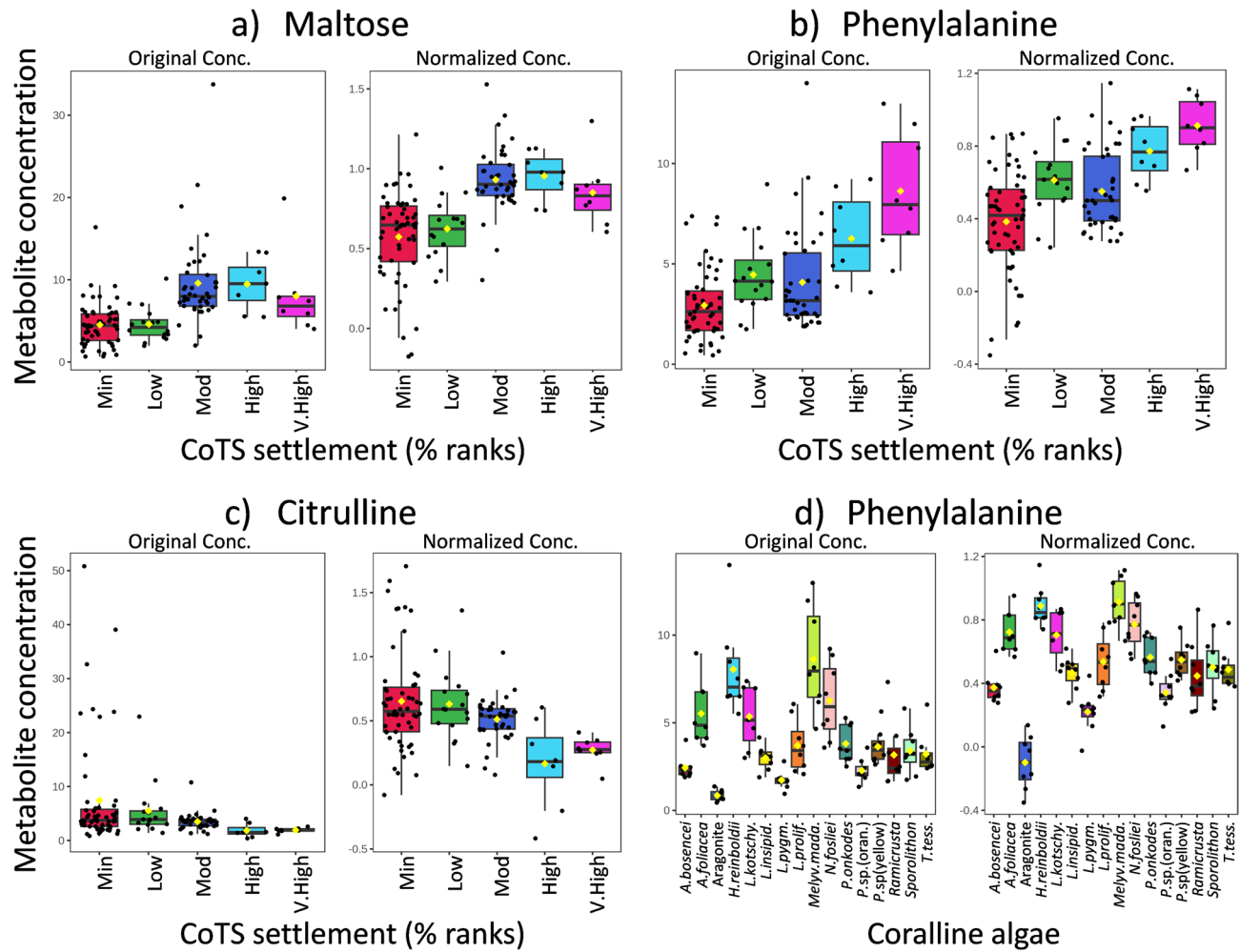


Fig. 7. Boxplots of relative concentrations (spectral bins) of metabolites across a gradient of CoTS settlement (a–c) and coralline algae species (d). (a) Maltose; (b) Phenylalanine 7.3461; (c) Citrulline; and (d) Phenylalanine 7.3461 vs. coralline algae species. Bar plots on the left show the original values (mean \pm SD) and the box and whisker plots on the right show the normalised values. All metabolites are significantly correlated with settlement (see text for details).

lineages tend to possess a reduced diversity of metabolites compared to more recently evolved and structurally complex taxa^{40,41}. A similar pattern may be operating in Corallinophycidae. Recent studies support this hypothesis by revealing that monosaccharides richness (and diversity) in cell walls is lower in *Sporolithon* cf. *durum* compared to that from species in Hapalidiales and Corallinales⁴². Moreover, *S. cf. durum* has shown a more limited transcriptomic response to environmental change than Corallinales⁴³, suggesting lower metabolic plasticity and complexity in Sporolithales.

Despite the general clustering of samples within taxonomic families, there was distinct metabolic divergence among species within the same genus and between genera within the same subfamily. This was particularly evident in the Metagonioliethoideae, which included three species of *Porolithon*, and in the Lithophylloideae, which included three species of *Lithophyllum* and *Titanoderma* (Supplementary Fig. S2; Supplementary Table S4). In the case of *Porolithon*, the three species are considered cryptic as they lack clear morpho-anatomical characters and cannot be distinguished (i.e. they all look the same) but are under different evolutionary trajectories, yet they exhibit distinct metabolite profiles. These chemical differences may reflect divergent evolutionary trajectories, suggesting that selection is acting on chemical and metabolic pathways rather than on morpho-anatomy. This observation aligns with the idea that highly diverse ecosystems like coral reefs promote chemical diversity⁴⁴, and suggest that environmental pressures such as herbivory and space competition may drive metabolic differentiation in the absence of visible morphological change.

Potential influence of the environment on metabolomic profiles

The environment seems to exert an important influence in shaping the metabolomes of the studied species. In particular, metabolic profiles from the shallow, well-lit environments were significantly different from those of the cryptic, low light environments, consistent with the findings from French Polynesia²³. However, these patterns should be interpreted with caution, as species composition is not independent of habitat type. In other

words, the observed metabolomic differences may partly reflect phylogenetic or species-specific effects rather than environmental influence alone. For example, species of *Porolithon* are typically associated with shallow, high irradiance reef crest environments⁴⁵, and exhibit distinct metabolic profiles that may be a result of both evolutionary history and environmental exposure. Conversely, species such as *Ramicrusta*, *Lithothamnion* and *Sporolithon* are generally restricted to caves or shaded microhabitats and are generally excluded from environments with high irradiance^{25,46,47}. This habitat-specific distribution complicates direct attribution of metabolomic differences to environmental factors such as irradiance. To disentangle species and environmental effects, reciprocal transplant experiments using the same species of alga (confirmed using DNA sequencing) would help elucidate the direct influence of environmental conditions on CCA metabolomes. Despite this limitation of the current dataset, our results reveal distinct chemical fingerprints from different habitats and light environments, offering a valuable foundation for generating hypotheses about the environmental regulation of CCA metabolism and function.

Several metabolites in our study may also be linked to light intensity regimes. For instance, glycylproline (dipeptide composed of two amino acids: glycine and proline), which may be involved in UV protection (glycine is a mycosporine-like amino acids ultra-violet-absorbing compound)⁴⁸, was more abundant in species from high-light environments. Confirmation of this role, however, requires further analyses of the compound's absorption spectrum. Conversely, the accumulation of citrulline, may suggest roles in nitrogen metabolism and storage under reduced irradiance⁴⁹. These preliminary associations highlight the need for targeted studies to investigate the ecological and physiological functions of key metabolites under variable environmental conditions.

Relationship between CCA metabolites and coral settlement

Our study demonstrates that the relationship between coral settlement and CCA metabolomes is highly variable and species-specific, both in terms of coral and algal identity. Given the large number of coral-algal combinations examined, this variability is not unexpected. The intensity of settlement for some coral groups was related to distinct chemical profiles, suggesting that complex compound mixtures can modulate settlement behaviour. For example, strong associations were found between metabolic profiles and settlement intensity for Acroporidae, particularly *Acropora hyacinthus* (Fig. 4), while preferences for other species, such as *Platygyra sinensis*, were less clear. These findings support previous research highlighting variable coral larval responses to chemical cues from CCA⁵⁰.

Titanoderma has long been considered a model CCA for inducing coral settlement, known to elicit high larval settlement on its surface across multiple reef systems in the Caribbean and Indo-Pacific^{19,23–25,51,52}. In our study, and based on inspection of heatmaps visualising the relative concentrations of metabolites (Fig. 2), the metabolome of *Titanoderma cf. tessellatum* was characterised by an overall relative depletion of many metabolites, but was moderately enriched in betaine (Fig. 2). It remains unclear whether this apparent depletion itself plays a role in enhancing larval attraction, or if specific enriched metabolites are the key drivers. In French Polynesia, the metabolome of *Titanoderma "prototypum"* was enriched in glycerolipids, including betaine lipids²³, while Tebben et al.¹⁸ identified glycoglycerolipids and polysaccharides from the CCA *Porolithon cf. onkodes* as primary constituents of settlement inducing fractions in *Acropora* spp.¹⁸. These findings highlight glycerolipids, including betaine lipids, as a key chemical class potentially underpinning coral larval settlement, and our study provides novel evidence of specific betaine compounds (such as glycine betaine) (Figs. 5 and 6) that may underpin coral larval settlement behaviour.

Several polysaccharides, including the disaccharide maltose and the trisaccharide raffinose, were positively correlated with coral settlement (Fig. 5). These sugars may function as chemical cues that signal a favourable microhabitat or metabolic resource to larvae. Carbohydrates and carbohydrate conjugates such as sulfated glycosaminoglycans⁵³ and uncharacterised polysaccharides^{18,50} have been previously extracted from CCA and proposed as inducers for coral settlement^{18,53}. Our use of untargeted metabolomics with H-NMR allowed the identification of specific, potentially bioactive sugars, which may act individually or in conjunction with other metabolites to influence larval behaviour in both coral and CoTS larvae. These compounds, as well as betaine, are also rich in essential nutrients such as carbon and nitrogen, which may support early microbial colonisation or larval metabolism. Other metabolomic studies have shown that CCA and *Ramicrusta* exude complex mixtures of metabolites that influence microbial communities on coral reefs^{31,37}. It is plausible that larvae detect these compounds as indicators of a suitable settlement substrate, either directly, or indirectly via microbial biofilms, or perhaps as an initial energy source while symbionts are acquired.

Our study does not allow us to determine whether the detected metabolites are produced directly by the coralline algae tissue or by the microbial biofilms associated to the algae surface. Nonetheless, it is worth considering the potential role of CCA-associated microbes in coral settlement. Compounds previously isolated from CCA-associated bacteria and known to induce coral settlement, such as tetrabromopyrrole (TPB)^{22,54,55} and cycloprodigiosin (CYPRO)^{56,57}, were not detected in our study. However, we cannot rule out the possibility that some of the unidentified features reported (Supplementary Table S2) may be related to these or similar bioactive molecules, underscoring the need for further investigations into the identity of the CCA-derived metabolites and the detection limits influencing metabolite identification. There is ongoing debate about whether coral (or CoTS) settlement-inducing chemical cues are produced by the CCA tissue^{18,19,58} or by the microbial biofilms^{20–22,58}. Different CCA species harbour distinct microbiomes^{58,59}, and there are close associations between CCA-associated microbiomes and tissue-associated metabolomes^{23,34}. Therefore it is likely that complex interactions between host metabolomes and microbial communities strongly influence coral settlement outcomes^{19,23,27}. Further investigations are required to elucidate the mechanisms by which specific CCA compounds influence microbial communities (or vice versa) to modulate coral settlement.

Relationship between CCA metabolites and CoTS settlement

Compared to coral larvae, CCA are not only important in inducing settlement and indicating ‘suitable’ environmental conditions, but also provide the first food source of CoTS prior to their ontogenetic diet shift to coral after ~ 6 months⁶⁰. Our study identified a suite of compounds, including carbohydrates such as maltose, raffinose and the amino acid phenylalanine, that were positively correlated with CoTS larval settlement. There was no clear metabolic profile associated to high settlement of CoTS; however, these compounds were enriched in several CCA species, including *Melyvonnea cf. madagascariensis*. This species has previously been shown to induce very high settlement in *Acanthaster cf. solaris*⁸ and is preferentially consumed by juvenile CoTS, supporting faster growth rates⁶⁰. Betaine, known to act as an effective feeding cue for adult *Acanthaster* spp.^{61,62}, was also moderately enriched in *M. cf. madagascariensis*. It is possible that high concentrations of carbohydrates like maltose, increase the nutritional value of the CCA and thus lead to accelerated growth of juveniles and earlier transition to coral feeding^{60,63}. An earlier ontogenetic shift to coral feeding may assist juvenile CoTS to escape high predation rates on small-bodied, herbivorous juveniles⁶⁴, thus contributing to population outbreaks. The enrichment of phenylalanine is noteworthy, as this amino acid could potentially serve as a precursor to secondary metabolites such as alkaloids or signalling compounds in CoTS larvae, though its specific role remains untested. The ecological function of these metabolites as attractants of CoTS settlement, recruitment and growth is still poorly understood and represents a promising area of future research⁶². Our study provides novel insights into the complex chemical mixture of compounds mediating larval settlement in CoTS. These findings could be applied to develop novel chemical-based strategies to attract CoTS larvae and juveniles and develop traps to contribute to strategies to control population outbreaks and reduce the impacts of this species in coral reefs⁶². Future studies determining the relative contribution of CCA chemical compounds and CCA-associated microbial biofilms as drivers of CoTS larval settlement and feeding behaviour, as well as the required cue concentrations will be important for the development of CoTS capture traps. Importantly, further insight into the prevalence and distribution of CCA, particularly *Melyvonnea cf. madagascariensis*, and their response to environmental changes may also assist us to understand (and manage) causes of CoTS outbreaks.

Conclusions

This study provides the most comprehensive analysis to date of coralline algal metabolomes and their ecological relevance to coral reef systems. While the suite of metabolomes presented here comprises many unknown features, providing future opportunities for discovery, we demonstrate that CCA metabolomes are highly variable across species, congruent to phylogenetic lineages and habitats at some level, and are likely shaped by both evolutionary history and environmental adaptation. Importantly, we reveal that specific metabolites, including disaccharides, trisaccharides, and betaine compounds, are positively associated with the larval settlement of reef-building corals and their primary predator, the crown-of-thorns starfish (CoTS). These findings not only deepen our understanding of the chemical ecology underpinning larval settlement processes on reefs, but also offer practical insights for reef restoration and pest management. Targeted application of these bioactive compounds could inform the design of improved coral aquaculture systems and the development of CoTS settlement and recruitment traps, contributing to integrated strategies to improve coral reef resilience.

Future research should aim to determine whether the proposed chemical compounds, individually or in combination, induce settlement in coral and CoTS larvae. Further investigations should assess how key CCA metabolites respond to environmental variation, and elucidate their role in larval settlement under different environmental conditions. In addition, identifying the specific sources of settlement-associated chemical cues and characterising the interrelationships between CCA metabolomes and CCA-associated microbiomes will provide insights into the chemical communications and how they influence coral and CoTS larval behaviour.

Methods

Field collections, taxonomic and molecular identification

The metabolomic analyses were conducted on 14 species of coralline red algae collected from shallow coral reefs around Davies Reef (18°49'13.5"S 147°38'40.32"E), and the Palm Island Group (18°45'56.4"S 146°32'2.58"E) in the central Great Barrier Reef (GBR). These reefs were selected due to their proximity to the headquarters of the Australian Institute of Marine Science (AIMS), where the coral and CoTS larval experiments were conducted^{8,25}. Davies Reef is representative of a low-turbidity mid-shelf reef, whereas the reefs of the Palm Island group typify the fringing reefs of inshore islands of the GBR. The CCA species chosen for this study are common and representative of the CCA communities in the region (e.g. ^{45,47}) and included members of the three main phylogenetic orders of tropical corallines (Subclass Corallinophycidae): Corallinales, Hapalidiales and Sporolithales. Further, the selected genera and species (Table 1) have important ecological relevance as they contribute to reef framework construction and cementation (e.g. *Porolithon* spp., *Lithophyllum* spp., *Neogoniolithon* cf. *fosliei*, *Hydrolithon* cf. *reinboldii*, *Adeylithon* cf. *bosencet*^{65,66} and induce the settlement of corals (e.g. *Titanoderna* cf. *tessellatum*, *Porolithon* spp.^{19,23,25}) and CoTS (e.g. *Melyvonnea cf. madagascariensis*, *Lithothamnion* spp.^{8,67}. Additionally, the calcareous alga *Ramicrusta* sp. (Subclass Rhodymeniophycidae) was included in the analyses. Although not a true coralline alga, *Ramicrusta* sp. shares several morphological and ecological characteristics with CCA, such as a calcified, encrusting thallus, and it plays important roles in coral reef ecosystems (e.g.⁶⁸). For comparative purposes, filamentous algal turfs growing on coral rubble were also collected and analysed.

Specimens were collected on SCUBA in October 2021 using hammer and chisel from reef crests and shallow reef slopes habitats (2–6 m depth), and from microenvironments such as crevices and overhangs and caves. Details of the taxonomic classification (orders, families, subfamilies), and reef habitat and light environment

of each of the 15 collected algal species, are provided in Table 1. Algal samples were collected under GBRMPA Permit G21/45348.1 through the AIMS.

Collected specimens were rapidly transferred to 68 L plastic bins (Nally, Australia) with running seawater and sorted by species onboard the AIMS research vessel 'Magnetic'. A total of 3,131 specimens were collected to provide material for the metabolomics study, the coral larval settlement experiments using 15 coral species (Abdul Wahab et al. 2023) and the CoTS larval settlement assays (Doll et al. 2023). Each specimen was carefully examined by GD-P under a stereomicroscope to confirm taxonomic identity, focusing on key diagnostic features typical of CCA genera and species. These included the presence and arrangement of trichocytes, multiporate conceptacles and sporangial sori, as well as the organisation of internal thallus (e.g., dimerous, monomerous or coaxial). 110 specimens were designated as herbarium specimens (numbers varied across species as some are more difficult to identify than others; Table 1) and dried using silica gel crystals; specimens were decalcified to confirm the presence of secondary pit connections and cell fusions, important traits for distinguishing between genera⁴⁷. Representative herbarium specimens were used for molecular identification (see section below) and archived in the Coral Reef Algae Lab collection at Griffith University, Brisbane.

Following initial sorting, CCA samples were transported to the AIMS National Sea Simulator (SeaSim) in Townsville on October 20th and placed in holding tanks (80 × 140 × 28 cm, 280 L) receiving 1 μm filtered seawater at a rate of ~ 3 turnovers per day. Lighting regimes were adjusted to match habitat specific light preferences: high-light adapted CCA received up to ~ 120 μmol photons m⁻² s⁻¹ at midday, while low-light adapted CCA were maintained under 12.7–15 μmol photons m⁻² s⁻¹. A 6.5 h linear ramp-up from darkness began at 05:30 h, followed by a 6.5-hour ramp-down to complete darkness at 18:30 h. Light intensities were measured using a LI-COR LI-250 A light meter.

For handling and transport, specimens were cut into 1 × 1 cm fragments and allowed to recover for 7–10 days. Eight replicate fragments were prepared per CCA species and for algal turf samples growing on coral rubble. Inert aragonite substrates were also included as controls. Each fragment was placed in a cryovial and flash-frozen in liquid nitrogen on November 12th. The samples could not be flash-frozen immediately after collection; thus, potential effects of aquarium conditions on the CCA metabolomes cannot be fully excluded. Nevertheless, given the high and stable water quality maintained at SeaSim, we are confident that the metabolomes accurately represent those of freshly collected specimens. Samples were subsequently shipped to Griffith University (Gold Coast) for metabolomic analyses (see below).

Molecular identification

The taxonomic identity of all CCA species and their phylogenetic relationships were determined by analyses of two genetic markers: psbA (psbAF1 and psbAR2 primers) and rbcL (F57/R1150 and F993/RrbcStart primers). DNA extraction and amplification was conducted by S Jeong (Griffith University, Nathan) following⁶⁹ and sequencing was performed by Macrogen (Seoul, South Korea). Further details of the DNA extractions and phylogenetic analyses and trees are provided in²⁵ and sequences are accessible in GenBank with accession numbers included in Table 1. The phylogenetic trees are useful to delineate groups (or clades) allowing us to explore the relationship between the evolutionary history of CCA and their metabolic profiles.

Metabolomics approach

The tissue associated metabolomes of the CCA were analysed using an untargeted metabolomic approach aimed at comprehensively detecting and identifying as many metabolites as possible. Nuclear Magnetic Resonance (NMR) spectroscopy was used for these analyses. Although NMR is less sensitive than platforms such as liquid chromatography mass spectrometry (LC-MS), it offers distinct advantages for structural elucidation of unknown compounds, particularly in organisms for which metabolite databases are limited (as discussed in^{70,71}).

Metabolites were extracted following established protocols^{72,73}. Briefly, 1 cm² CCA fragments were incubated overnight at -20 °C in 1.2 mL methanol. The following day, chloroform and water were added, and the mixture was vortexed, centrifuged and partitioned using a methanol: chloroform: water solvent system (4: 8: 3). This biphasic extraction effectively separates polar (water soluble) metabolites from non-polar (lipid soluble) compounds, while precipitating proteins and cellular debris.

Nuclear magnetic resonance (NMR) spectroscopy

Polar extracts were dried using a centrifugal evaporator, and metabolites were reconstituted in 200 μL deuterium oxide (D₂O) buffered with phosphate-buffered saline (PBS) and including 0.05% sodium-3-(trimethylsilyl)-2,2,3,3-tetradeuteriopropionate (TSP) as an internal reference. Reconstituted samples were loaded into 3 mm NMR tubes using a glass syringe (Hamilton[®] Company, Reno, Nevada), and spectra were acquired with an 800 MHz Bruker Avance III HDX spectrometer equipped with a Triple (TCI) Resonance 5 mm Cryoprobe. Spectra were acquired at 298 K, using the internal reference for field locking (TSP δ 0.00 ppm) and the zg30 pulse program with 0.8 relaxation delay, 8.20 pulse width and a spectral width of 16 kHz using 64 scans.

Acquired NMR spectra for each sample were manually phase corrected, baseline adjusted using the ablative algorithm, referenced and normalised to TSP (1H δ 0.00), using MestReNova version 14.2.2 (Mestrelab Research S.L., Spain). Metabolites were identified based on ¹H NMR spectra using Chenomx NMR Suite version 11 software (Chenomx Inc., Edmonton, Canada) (www.chenomx.com) and, where possible, additional annotations were made by cross-referencing against standard compounds in the Human Metabolome Database (HMDB) and Yeast Metabolome Database (YMDB).

Coral larvae and CoTS settlement

To explore the relationship between the CCA metabolomes and larval settlement in both corals and CoTS, we integrated metabolite abundance data generated in this study with published larval settlement data for 15 species

of scleractinian corals²⁵ and one species of CoTS (*Acanthaster cf. solaris*)⁸. Settlement assays were conducted in parallel with the metabolomic analyses using the same pool of CCA fragments, with all species collected at the same sites and times by the research team (GD-P, MAW) and prepared at the AIMS SeaSim facility. While the exact fragments used for metabolomic and settlement assays differed (to avoid any influence of larval exposure on the CCA metabolomes), the consistency of the metabolic profiles within each CCA species confirms that the larvae were exposed to the same suite of tissue associated metabolites analysed with NMR in this study.

The coral larval settlement methodology is described in Abdul Wahab et al. (2023)²⁵. In short, gravid corals from 15 coral species (across five families) were collected from the same reefs as the CCA samples and transported to the SeaSim. A list of the coral species used, with details of collection sites, modes of reproduction, spawning information, and the age of larvae at the start of the experiment is included in Table 1 of Abdul Wahab et al. (2023). After gamete release and fertilisation, embryos were transferred to culture tanks and raised until larvae were ready for use in settlement assays. Each assay was conducted in six-well cell culture plates containing 10 mL of 0.2 µm filtered seawater, with ten 10 actively swimming larvae and one live 5 × 5 mm CCA treatment fragment per well. Settlement was defined as permanent attachment and metamorphosis, either on live CCA tissue, on its underside or sides, within its matrix, or the plastic surface of the well. Except for a few cases, 12 replicate fragments per CCA species were used, and mean settlement success was calculated for subsequent correlations with metabolite data.

CoTS larval settlement assays are detailed in Doll et al. (2023)⁸, using the same CCA species and pool of fragments as the metabolite analyses. CoTS larvae were reared at the AIMS SeaSim following^{8,74}. For each settlement assay, 10 competent CoTS larvae were added to 6-well cell culture plates containing 10 mL of 0.2 µm filtered seawater and a single 5 × 5 mm live CCA treatment fragment. Twelve replicates were conducted per CCA treatment. The categorical, semiquantitative settlement data used in our analyses is based on the mean settlement success for each CCA treatment (i.e., mean percentage of settled CoTS larvae across 12 replicate assays) within 24 h following experiment commencement.

Peak assignments and processing of ^1H NMR spectra

Post processing was performed with MestReNova v11.0.3 (Mestrelab Research S.L., Spain). ^1H NMR FIDs were Fourier transformed with a 0.3 Hz line broadening and HSQC spectra were processed with default Bruker post-processing parameters. All spectra were manually phase corrected, automatically baseline adjusted (ablative) and referenced to TSP (1 H d 0.00, 13 C d 0.0). Spectra were normalized to the chemical reference and binned into 0.02 ppm buckets. Integrated peak areas of each bucket were exported for further processing and multivariate statistical analysis. Metabolites were tentatively assigned to ^1H NMR spectra using Chenomx NMR Suite version 11 software (Chenomx Inc., Edmonton, Canada) (www.chenomx.com). Metabolite identification was further verified by comparison of HSQC NMR spectra with published reference spectra from the Human Metabolome Database (HMDB) and Yeast Metabolome Database (YMDB).

Statistical analyses

Spectra data were investigated using multivariate analyses performed using MetaboAnalyst 6.0 (<https://www.metaboanalyst.ca/home.xhtml>)⁷⁵. Imported data were filtered using a reliability and variance filter (interquartile range) of 25% and 5% respectively, and no abundance filtering was applied. Data were log10 transformed and normalisation examined visually. We used separation [Principal Components Analysis (PCA)] and classification techniques [Partial Least Squares Discriminant Analysis (PLS-DA), sparse PLS-DA (sPLS-DA) and heatmaps] to explore differences in metabolite profiles between treatment groups (e.g. species, phylogenetic groups, habitat). We used PERMANOVA (Permutational Multivariate Analysis of Variance) to determine significant differences between groups in the PCA and distributions were computed using the Euclidean distance. PERMANOVA results, including FDR (False Discovery Rate)-adjusted p-values are presented in Supplementary Table S3-S5. PLS-DA is used to maximise separation among groups, while sPLS-DA can reduce the number of variables (metabolites) to produce robust and easy-to-interpret models. VIP (variable importance in projection) scores and Loading plots from the PLS-DA, and sPLS-DA, respectively were also inspected to help in identification of relevant compounds in each group under study; specifically, these plots show the contributions of compounds with high importance to the classification of the models. VIP score is a weighted sum of squares of the PLS loadings, and the weights are based on the amount of explained Y-variance in each dimension of the multivariate analysis (or model). The Loadings plot shows the compounds selected by the sPLS-DA model for a given component, and compounds are ranked by the absolute values of their loadings. For the PLS-DA, cross validation and permutation analyses were conducted and Q2, R2 (with a maximum of 5 components to search) and p values (1,000 permutations) are reported. sPLS-DA were run with 5 components and 10 variables within each component and Classification Error Rate (CER) are reported. Clustering in heatmaps was performed using Euclidean distance and the Ward method. The algal turfs and aragonite substrate treatments were initially considered in the analyses, but later removed to maximise data visualisation and trend identification within the coralline algae.

The relationship between the CCA chemical profiles with coral and CoTS settlement data was visually explored using PCA, PLS-DA, sPLS-DA and heatmaps, as well as using the Metadata module in MetaboAnalyst 6.0. Spearman rank correlations were used to evaluate the relationship between the spectral bins (similar to concentrations) of metabolites and percent settlement, and for this purpose settlement data (corals - Abdul Wahab et al. 2023, CoTS - Doll et al. 2023) was converted to a categorical, semiquantitative ranking (20% bins, 5 categories; 0–19% = minimal settlement; 20–39% = low, 40–59% = moderate, 60–79% = high, and 80–100% = very high) for a more conservative approach in the analyses. For total coral settlement, there were only 3 settlement categories (minimal, moderate and high) as those not included (low and very high) had a frequency of zero.

Data availability

The original feature spectral bin dataset generated during the current study is available in the Griffith University institutional repository (Griffith Research Online -GRO), with the following accession number: <https://doi.org/10.25904/1912/5818>. Metadata of the CCA species used during the current study are included in Table 1 in the main article. DNA sequences of the CCA species used during the current study were uploaded to GenBank under accession numbers OP830444 to OP830473, and accession numbers are also included in Table 1. GenBank sequences could be accessed here: <https://www.ncbi.nlm.nih.gov/genbank/>.

Received: 12 August 2025; Accepted: 19 November 2025

Published online: 02 December 2025

References

1. De'ath, G., Fabricius, K. E., Sweatman, H. & Puotinen, M. The 27-year decline of coral cover on the Great Barrier Reef and its causes. *Proc. Natl. Acad. Sci. USA* **109**, 17995–17999, (2012). <https://doi.org/10.1073/pnas.1208909109>
2. Hughes, T. P. et al. Global warming and recurrent mass bleaching of corals. *Nature* **543**, 373–377 (2017).
3. Cramer, K. L. et al. Widespread loss of Caribbean acroporid corals was underway before coral bleaching and disease outbreaks. *Sci. Adv.* **6**, eaax9395. <https://doi.org/10.1126/sciadv.aax9395> (2020).
4. Toth, L. T. et al. The potential for coral reef restoration to mitigate coastal flooding as sea levels rise. *Nat. Commun.* **14**, 2313. <https://doi.org/10.1038/s41467-023-37858-2> (2023).
5. Morse, D. E., Hooker, N., Morse, A. N. C. & Jensen, R. A. Control of larval metamorphosis and recruitment in sympatric agariciid corals. *J. Exp. Mar. Biol. Ecol.* **116**, 193–217 (1988).
6. Heyward, A. J. & Negri, A. P. Natural inducers of coral larval metamorphosis. *Coral Reefs* **18**, 273–279 (1999).
7. Diaz-Pulido, G., Harii, S. & McCook, L. J. Hoegh-Guldberg, O. The impact of benthic algae on the settlement of a reef-building coral. *Coral Reefs* **29**, 203–208 (2010).
8. Doll, P. C. et al. Settlement cue selectivity by larvae of the destructive crown-of-thorns starfish. *Biol. Lett.* **19**, 20220399. <https://doi.org/10.1098/rsbl.2022.0399> (2023).
9. Doll, P. C. et al. Larval settlement in echinoderms: a review of processes and patterns. *Oceanogr. Mar. Biol. Annu. Rev.* **60**, 433–494 (2022).
10. Morse, A. N. C. & Morse, D. E. Recruitment and metamorphosis of *Haliotis* larvae induced by molecules uniquely available at the surfaces of crustose red algae. *J. Exp. Mar. Biol. Ecol.* **75**, 191–215 (1984).
11. Pawlik, J. R. Chemical ecology of the settlement of benthic marine invertebrates. *Oceanogr. Mar. Biol. Annu. Rev.* **30**, 273–335 (1992).
12. Nash, M. C., Diaz-Pulido, G., Harvey, A. S. & Adey, W. Coralline algal calcification: A morphological and process-based understanding. *PLoS ONE* **14**, e0221396. <https://doi.org/10.1371/journal.pone.0221396> (2019).
13. Nunn, P. D. Role of *Porolithon* algal-ridge growth in the development of the windward coast of Tongatapu Island, Tonga, South Pacific. *Earth Surf. Processes Land.* **18**, 427–439. <https://doi.org/10.1002/esp.3290180505> (1993).
14. Cornwall, C. E. et al. Crustose coralline algae can contribute more than corals to coral reef carbonate production. *Commun. Earth Environ.* **4**, 105. <https://doi.org/10.1038/s43247-023-00766-w> (2023).
15. Kenyon, T. M. et al. Trajectories and agents of binding in stabilized and unstabilized coral rubble across environmental gradients. *Ecosphere* **16**, e70195. <https://doi.org/10.1002/ecs2.70195> (2025).
16. Aguirre, J. & Braga, J. C. Rhodolith beds in a shifting world: A palaeontological perspective. *Aquat. Conserv. Mar. Freshw. Ecosyst.* **34**, e70015. <https://doi.org/10.1002/aqc.70015> (2024).
17. Schubert, N. et al. Pink power—the importance of coralline algal beds in the oceanic carbon cycle. *Nat. Commun.* **15**, 8282. <https://doi.org/10.1038/s41467-024-52697-5> (2024).
18. Tebben, J. et al. Chemical mediation of coral larval settlement by crustose coralline algae. *Sci. Rep.* **5**, 10803 (2015).
19. Gómez-Lemos, L. A., Doropoulos, C., Bayraktarov, E. & Diaz-Pulido, G. Coralline algal metabolites induce settlement and mediate the inductive effect of epiphytic microbes on coral larvae. *Sci. Rep.* **8**, 17557. <https://doi.org/10.1038/s41598-018-35206-9> (2018).
20. Negri, A. P., Webster, N. S., Hill, R. T. & Heyward, A. J. Metamorphosis of broadcast spawning corals in response to bacteria isolated from crustose algae. *Mar. Ecol. Prog. Ser.* **223**, 121–131 (2001).
21. Webster, N. S. et al. Metamorphosis of a scleractinian coral in response to microbial biofilms. *Appl. Environ. Microbiol.* **70**, 1213–1221. <https://doi.org/10.1128/AEM.70.2.1213-1221.2004> (2004).
22. Snead, J. M., Sharp, K. H., Ritchie, K. B. & Paul, V. J. The chemical cue tetrabromopyrrole from a biofilm bacterium induces settlement of multiple Caribbean corals. *Proc. R. Soc. Ser. B Biol. Sci.* **281**, 2013086 <https://doi.org/10.1098/rspb.2013.3086> (2014).
23. Jorissen, H. et al. Coral larval settlement preferences linked to crustose coralline algae with distinct chemical and microbial signatures. *Sci. Rep.* **11**, 14610. <https://doi.org/10.1038/s41598-021-94096-6> (2021).
24. Price, N. Habitat selection, facilitation, and biotic settlement cues affect distribution and performance of coral recruits in French Polynesia. *Oecologia* **163**, 747–758 (2010).
25. Abdul Wahab, M. A. et al. Hierarchical settlement behaviours of coral larvae to common coralline algae. *Sci. Rep.* **13**, 5795. <https://doi.org/10.1038/s41598-023-32676-4> (2023).
26. Ritson-Williams, R., Arnold, S. N., Paul, V. J. & Steneck, R. S. Larval settlement preferences of *Acropora palmata* and *Montastraea faveolata* in response to diverse red algae. *Coral Reefs* **33**, 59–66 (2014).
27. Quinlan, Z. A. et al. Coral larval settlement induction using tissue-associated and exuded coralline algae metabolites and the identification of putative chemical cues. *Proc. R. Soc. Ser. B Biol. Sci.* **290**, 20231476 <https://doi.org/10.1098/rspb.2023.1476> (2023).
28. Kundu, S. et al. Biomimetic chemical microhabitats enhance coral settlement. *Trends Biotechnol.* **43**, 2232–2250. <https://doi.org/10.1016/j.tibtech.2025.03.019> (2025).
29. Motti, C. A. et al. Deployment of semiochemical control agents to manage Crown-of-Thorns starfish populations. A report to the Australian Government by the COTS Control Innovation Program, Townsville, Australia. **80** (2022).
30. Birkeland, C. Terrestrial runoff as a cause of outbreaks of *Acanthaster planci* (Echinodermata: Asteroidea). *Mar. Biol.* **69**, 175–185. <https://doi.org/10.1007/BF00396897> (1982).
31. Wegley Kelly, L. et al. Distinguishing the molecular diversity, nutrient content, and energetic potential of exometabolomes produced by macroalgae and reef-building corals. *Proc. Natl. Acad. Sci. USA* **119** (e2110283119). <https://doi.org/10.1073/PNAS.2110283119> (2022).
32. Vizon, C. et al. The metabolome of crustose coralline algae is driven by phylogeny and environmental conditions. *Algal Res.* **90**, 104146. <https://doi.org/10.1016/j.algal.2025.104146> (2025).
33. Quinn, R. A. et al. Metabolomics of reef benthic interactions reveals a bioactive lipid involved in coral defence. *Proc. R. Soc. Ser. B Biol. Sci.* **283**, 20160469 <https://doi.org/10.1098/rspb.2016.0469> (2016).
34. Mannochio-Russo, H. et al. Microbiomes and metabolomes of dominant coral reef primary producers illustrate a potential role for immunolipids in marine symbioses. *Commun. Biol.* **6**, 896. <https://doi.org/10.1038/s42003-023-05230-1> (2023).

35. Wegley Kelly, L., Haas, A. F. & Nelson, C. E. Ecosystem microbiology of coral reefs: linking genomic, metabolomic, and biogeochemical dynamics from animal symbioses to reefscape processes. *mSystems* **3**, e00162–e00117. <https://doi.org/10.1128/mSystems.00162-17> (2018).
36. Guiry, M. D. & Guiry, G. M. *AlgaeBase. World-wide electronic publication*. <https://www.algaebase.org> (2025).
37. Weber, L. et al. Benthic exometabolites and their ecological significance on threatened Caribbean coral reefs. *ISME Commun.* **2**, 101. <https://doi.org/10.1038/s43705-022-00184-7> (2022).
38. Aguirre, J., Riding, R. & Braga, J. C. Diversity of coralline red algae: origination and extinction patterns from the Early Cretaceous to the Pleistocene. *Paleobiology* **26**, 651–667. [https://doi.org/10.1666/0094-8373\(2000\)026%3C0651:DOCRAO%3E2.0.CO;2](https://doi.org/10.1666/0094-8373(2000)026%3C0651:DOCRAO%3E2.0.CO;2) (2000).
39. Peña, V. et al. Radiation of the coralline red algae (Corallinophycidae, Rhodophyta) crown group as inferred from a multilocus time-calibrated phylogeny. *Mol. Phylogen Evol.* **150**, 106845. <https://doi.org/10.1016/j.ympev.2020.106845> (2020).
40. Weng, J. K. The evolutionary paths towards complexity: a metabolic perspective. *New. Phytol.* **201**, 1141–1149. <https://doi.org/10.1111/nph.12416> (2014).
41. Dadras, A. et al. Accessible versatility underpins the deep evolution of plant specialized metabolism. *Phytochem Rev.* **24**, 13–26. <https://doi.org/10.1007/s11101-023-09863-2> (2025).
42. Bergstrom, E. et al. Cell wall organic matrix composition and biomineralization across reef-building coralline algae under global change. *J. Phycol.* **59**, 111–125. <https://doi.org/10.1111/jpy.13290> (2023).
43. Page, T. M., McDougall, C., Bar, I. & Diaz-Pulido, G. Transcriptomic stability or lability explains sensitivity to climate stressors in coralline algae. *BMC Genom.* **23**, 729. <https://doi.org/10.1186/s12864-022-08931-9> (2022).
44. Hartmann, A. C. et al. Meta-mass shift chemical profiling of metabolomes from coral reefs. *Proc. Natl. Acad. Sci. USA* **114**, 11685–11690. <https://doi.org/10.1073/pnas.1710248114> (2017).
45. Dean, A. J., Steneck, R. S., Tager, D. & Pandolfi, J. M. Distribution, abundance and diversity of crustose coralline algae on the Great Barrier Reef. *Coral Reefs* **34**, 581–594. <https://doi.org/10.1007/s00338-015-1263-5> (2015).
46. Adey, W. H., Townsend, R. A. & Boykins, W. T. The crustose coralline algae (Rhodophyta: Corallinaceae) of the Hawaiian Islands. *Smithson. Contrib. Mar. Sci.* **15**, 1–74 (1982).
47. Ringeltaube, P. & Harvey, A. Non-geniculate coralline algae (Corallinales, Rhodophyta) on Heron reef, Great Barrier Reef (Australia). *Bot. Mar.* **43**, 431–454 (2000).
48. Sun, Y. et al. Distribution, contents, and types of mycosporine-like amino acids (MAAs) in marine macroalgae and a database for MAAs based on these characteristics. *Mar. Drugs* **18**, 43. <https://doi.org/10.3390/MD18010043> (2020).
49. Costanzo, S. D., O'Donohue, M. J. & Dennison, W. C. *Gracilaria Edulis* (Rhodophyta) as a biological indicator of pulsed nutrients in oligotrophic waters. *J. Phycol.* **36**, 680–685. <https://doi.org/10.1046/j.1529-8817.2000.99180.x> (2000).
50. Whitman, T. N., Negri, A. P., Bourne, D. G. & Randall, C. J. Settlement of larvae from four families of corals in response to a crustose coralline alga and its biochemical morphogens. *Sci. Rep.* **10**, 16397. <https://doi.org/10.1038/s41598-020-73103-2> (2020).
51. Harrington, L., Fabricius, K. E., De'ath, G. & Negri, A. P. Recognition and selection of settlement substrata determine post-settlement survival in corals. *Ecology* **85**, 3428–3437 (2004).
52. Alvarado-Chacón, E. M. et al. Early life history of the Caribbean coral *Orbicella faveolata* (Scleractinia: Merulinidae). *Rev. Biol. Trop.* **68**, 1262–1274 (2020).
53. Morse, D. E. & Morse, A. N. C. Enzymatic characterization of the morphogen recognized by *Agaricia humilis* (Scleractinian coral) larvae. *Biol. Bull.* **181**, 104–122 (1991).
54. Tebben, J. et al. Induction of larval metamorphosis of the coral *Acropora millepora* by tetrabromopyrrole isolated from a *Pseudoalteromonas* bacterium. *PLoS One* **6**, e19082 (2011).
55. Sneed, J. M. et al. Coral settlement induction by tetrabromopyrrole is widespread among Caribbean corals and compound specific. *Front. Mar. Sci.* **10**, 1298518. <https://doi.org/10.3389/fmars.2023.1298518> (2024).
56. Petersen, L. E. et al. Mono- and multispecies biofilms from a crustose coralline alga induce settlement in the scleractinian coral *Leptastrea purpurea*. *Coral Reefs* **40**, 381–394. <https://doi.org/10.1007/s00338-021-02062-5> (2021).
57. Fiegel, L. J. et al. Cycloprodigiosin: A multispecies settlement cue for scleractinian coral larvae. *Sci. Rep.* **15** <https://doi.org/10.1038/s41598-025-12409-5> (2025).
58. Giorgi, A., Monti, M., Paul, V. J., Sneed, J. M. & Olson, J. B. Larvae from three Caribbean corals settle differently in response to crustose coralline alga and their bacterial communities. *Mar. Ecol. Prog. Ser.* **751**, 53–69 (2024).
59. Hochart, C. et al. High diversity of crustose coralline algae microbiomes across species and islands, and implications for coral recruits. *Environ. Microbiome* **19**, 112. <https://doi.org/10.1186/s40793-024-00640-y> (2024).
60. Jensen, K. et al. Feeding preferences and growth in herbivorous juvenile crown-of-thorns sea stars (*Acanthaster cf. solaris*). *Mar. Biol.* **172** <https://doi.org/10.1007/s00227-025-04646-z> (2025).
61. Schupp, P. & Bruckner, A. W. Management of *Acanthaster planci* breakouts through monitoring and use of *Acanthaster* feeding attractants/deterrents. Final Report, NOAA. (2008).
62. Harris, R. J. et al. The future of utilising semiochemical pest control methods to manage the destructive crown-of-thorns starfish outbreaks on coral reefs. *Biol. Conserv.* **302**, 110984. <https://doi.org/10.1016/j.biocon.2025.110984> (2025).
63. Llarena, D., Gomez-Cabrera, M. C., Doll, P. C. & Uthicke, S. Diet of herbivorous juveniles modulates growth, survival, and the timing of the ontogenetic diet shift to corallivory in crown-of-thorns sea stars. *Coral Reefs*. <https://doi.org/10.1007/s00338-025-0783-x> (2025).
64. Wolfe, K. et al. eDNA confirms lower trophic interactions help to modulate population outbreaks of the notorious crown-of-thorns sea star. *Proc. Natl. Acad. Sci. USA* **122**, e2424560122. <https://doi.org/10.1073/pnas.2424560122> (2025).
65. Dechnik, B. et al. The evolution of the Great Barrier Reef during the last interglacial period. *Global Planet. Change* **149**, 53–71. <https://doi.org/10.1016/j.gloplacha.2016.11.018> (2017).
66. Peña, V., Le Gall, L., Rösler, A., Payri, C. E. & Braga, J. C. *Adehylithon bosencei* gen. et sp. nov. (Corallinales, Rhodophyta): a new reef-building genus with anatomical affinities with the fossil *Aethesolithon*. *J. Phycol.* **55**, 134–145 (2019).
67. Johnson, C. R., Sutton, D. C., Olson, R. R. & Giddins, R. Settlement of crown-of-thorns starfish: role of bacteria on surfaces of coralline algae and a hypothesis for deepwater recruitment. *Mar. Ecol. Prog. Ser.* **71**, 143–162 (1991).
68. Edmunds, P. J., Schils, T. & Wilson, B. The rising threat of peysonnelioid algal crusts on coral reefs. *Curr. Biol.* **33**, R1140–R1141. <https://doi.org/10.1016/j.cub.2023.08.097> (2023).
69. Jeong, S. Y. et al. New branched *Porolithon* species (Corallinales, Rhodophyta) from the Great Barrier Reef, Coral Sea, and Lord Howe Island. *J. Phycol.* **59**, 1179–1201. <https://doi.org/10.1111/jpy.13387> (2023).
70. Kumar, M., Kuzhiumparambil, U., Pernice, M., Jiang, Z. & Ralph, P. J. Metabolomics: an emerging frontier of systems biology in marine macrophytes. *Algal Res.* **16**, 76–92. <https://doi.org/10.1016/j.algal.2016.02.033> (2016).
71. Lohr, K. E. et al. Metabolomic profiles differ among unique genotypes of a threatened Caribbean coral. *Sci. Rep.* **9**, 6067. <https://doi.org/10.1038/s41598-019-42434-0> (2019).
72. Beckonert, O. et al. Metabolic profiling, metabolomic and metabolomic procedures for NMR spectroscopy of urine, plasma, serum and tissue extracts. *Nat. Protoc.* **2**, 2692–2703. <https://doi.org/10.1038/nprot.2007.376> (2007).
73. Melvin, S. D., Lanctöt, C. M., Doriean, N. J. C., Carroll, A. R. & Bennett, W. W. Untargeted NMR-based metabolomics for field-scale monitoring: Temporal reproducibility and biomarker discovery in mosquitofish (*Gambusia holbrookii*) from a metal(lloid)-contaminated wetland. *Environ. Pollut.* **243**, 1096–1105. <https://doi.org/10.1016/j.envpol.2018.09.071> (2018).

74. Uthicke, S. et al. Climate change as an unexpected co-factor promoting coral eating seastar (*Acanthaster planci*) outbreaks. *Sci. Rep.* **5**, 8402. <https://doi.org/10.1038/srep08402> (2015).
75. Pang, Z. et al. MetaboAnalyst 6.0: towards a unified platform for metabolomics data processing, analysis and interpretation. *Nucleic Acids Res.* **52**, W398–W406. <https://doi.org/10.1093/nar/gkae253> (2024).

Acknowledgements

We would like to acknowledge and pay our respects to the Bindal and Wulguru kabba people, the Traditional Custodians of the land and sea country on which this research was performed. We thank Soyoung Jeong for the DNA extractions and sequencing.

Author contributions

G.D.-P. and M.A.A.W. conceptualized the study. SM performed the NMR analyses. M.A.A.W., S.F., AS, P.D., S.U., A.N. provided the larval settlement data. GD-P performed the data analyses, prepared figures/tables and drafted the manuscript. All authors revised the manuscript and approved the final draft.

Funding

This study was supported by the Reef Restoration and Adaptation Program, which aims to develop effective interventions to help the Reef resist, adapt and recover from the impacts of climate change, and which is funded by the partnership between the Australian Governments Reef Trust and the Great Barrier Reef Foundation. We thank the Australian Biological Resource Study (ABRS; grant no. RG19-35) for support to GDP.

Declarations

Competing interests

The authors declare no competing interests.

Additional information

Supplementary Information The online version contains supplementary material available at <https://doi.org/10.1038/s41598-025-29875-6>.

Correspondence and requests for materials should be addressed to G.D.-P.

Reprints and permissions information is available at www.nature.com/reprints.

Publisher's note Springer Nature remains neutral with regard to jurisdictional claims in published maps and institutional affiliations.

Open Access This article is licensed under a Creative Commons Attribution-NonCommercial-NoDerivatives 4.0 International License, which permits any non-commercial use, sharing, distribution and reproduction in any medium or format, as long as you give appropriate credit to the original author(s) and the source, provide a link to the Creative Commons licence, and indicate if you modified the licensed material. You do not have permission under this licence to share adapted material derived from this article or parts of it. The images or other third party material in this article are included in the article's Creative Commons licence, unless indicated otherwise in a credit line to the material. If material is not included in the article's Creative Commons licence and your intended use is not permitted by statutory regulation or exceeds the permitted use, you will need to obtain permission directly from the copyright holder. To view a copy of this licence, visit <http://creativecommons.org/licenses/by-nc-nd/4.0/>.

© The Author(s) 2025